

# Optimization of Radially Heterogeneous 1000-MW(e) LMFBR Core Configurations

## Volume 2: Appendixes A and B

**EPRI**

EPRI NP-1000  
Volume 2  
Project 620-25  
Interim Report  
November 1979

Keywords:

LMFBR Core  
HCDA  
Heterogeneous Core  
No Void Coefficient  
Bull's-Eye Core

**MASTER**

Prepared by  
Argonne National Laboratory  
Argonne, Illinois

DISTRIBUTION OF THIS DOCUMENT IS UNLIMITED

**ELECTRIC POWER RESEARCH INSTITUTE**

## **DISCLAIMER**

**This report was prepared as an account of work sponsored by an agency of the United States Government. Neither the United States Government nor any agency Thereof, nor any of their employees, makes any warranty, express or implied, or assumes any legal liability or responsibility for the accuracy, completeness, or usefulness of any information, apparatus, product, or process disclosed, or represents that its use would not infringe privately owned rights. Reference herein to any specific commercial product, process, or service by trade name, trademark, manufacturer, or otherwise does not necessarily constitute or imply its endorsement, recommendation, or favoring by the United States Government or any agency thereof. The views and opinions of authors expressed herein do not necessarily state or reflect those of the United States Government or any agency thereof.**

## **DISCLAIMER**

**Portions of this document may be illegible in electronic image products. Images are produced from the best available original document.**

# Optimization of Radially Heterogeneous 1000-MW(e) LMFBR Core Configurations

## Volume 2: Appendixes A and B

### NP-1000, Volume 2 Research Project 620-25

Interim Report, November 1979

Prepared by

ARGONNE NATIONAL LABORATORY  
Applied Physics Division  
EBR-II Division  
9700 South Cass Avenue  
Argonne, Illinois 60439

Principal Investigators

W. P. Barthold  
Y. Orehwa  
S. F. Su  
E. Hutter  
R. V. Batch  
J. C. Beitel  
R. B. Turski  
P. S. K. Lam

DISCLAIMER

This book was prepared as an account of work sponsored by an agency of the United States Government. Neither the United States Government nor any agency thereof, nor any of their employees, makes any warranty, express or implied, or assumes any legal liability or responsibility for the accuracy, completeness, or usefulness of any information, apparatus, product, or process disclosed, or represents that its use would not infringe privately owned rights. Reference herein to any specific commercial product, process, or service by trade name, trademark, manufacturer, or otherwise does not necessarily constitute or imply its endorsement, recommendation, or favoring by the United States Government or any agency thereof. The views and opinions of authors expressed herein do not necessarily state or reflect those of the United States Government or any agency thereof.

Prepared for

Electric Power Research Institute  
3412 Hillview Avenue  
Palo Alto, California 94304

EPRI Project Manager  
Edward L. Fuller  
Nuclear Power Division

*ef*  
DISTRIBUTION OF THIS DOCUMENT IS UNLIMITED

## ORDERING INFORMATION

Requests for copies of this report should be directed to Research Reports Center (RRC), Box 50490, Palo Alto, CA 94303, (415) 961-9043. There is no charge for reports requested by EPRI member utilities and affiliates contributing nonmembers, U.S. utility associations, U.S. government agencies (federal, state, and local), media, and foreign organizations with which EPRI has an information exchange agreement. On request, RRC will send a catalog of EPRI reports.

~~Copyright © 1989 Electric Power Research Institute, Inc.~~

EPRI authorizes the reproduction and distribution of all or any portion of this report and the preparation of any derivative work based on this report in each case on the condition that any such reproduction, distribution, and preparation shall acknowledge this report and EPRI as the source.

## NOTICE

This report was prepared by the organization(s) named below as an account of work sponsored by the Electric Power Research Institute, Inc. (EPRI). Neither EPRI members nor the organization(s) named below nor any person acting on their behalf (a) makes any warranty or representation, express or implied, with respect to the accuracy, completeness, or usefulness of the information contained in this report or that the use of any information, apparatus, method, or process disclosed in this report may not infringe privately owned rights, or (b) assumes any liabilities with respect to the use of, or for damages resulting from the use of, any information, apparatus, method, or process disclosed in this report.

Prepared by  
Argonne National Laboratory  
Argonne, Illinois

## EPRI PERSPECTIVE

### PROJECT DESCRIPTION

A hypothetical core disruptive accident (HCDA) and the impact it might cause, particularly on the underside of the head of a liquid metal fast breeder reactor (LMFBR) is a controversial issue. The debate is how much capability for safe absorption of impact energy must be designed into the reactor vessel and head. Neutronics and thermo-hydraulics analysts and core designers are the ones to whom this report is directed. Reactor vendors of early large-size LMFBRs can use this work as a sound starting base for improvements. The immediate application of this work is to provide the core design for the prototype large breeder reactor design studies conducted under EPRI Research Project 620.

This work, "Optimization of Radially Heterogeneous 1000-MW(e) LMFBR Core Configurations," is presented in four volumes. These are as follows:

- Volume 1: Design and Performance of Reference Cores
- Volume 2: Appendix A--Design Assumptions and Constraints  
Appendix B--Radially Heterogeneous Core Configurations
- Volume 3: Appendix C--Optimization of Core Performance Parameters
- Volume 4: Appendix D--Optimization of Core Configurations  
Appendix E--Component Designs

### PROJECT OBJECTIVES

The objective of the work reported here is to make the characteristics of large cores such that the impact energy of an HCDA would approach zero. Without special provisions, an LMFBR vessel and head will have greater impact resistance than would be needed by such a core, thus relieving the controversy and assuring a safe design feature.

This report presents the results of the second of three phases of effort to optimize a radial heterogeneous 1000-MW(e) LMFBR core design that will minimize energetics in

an HCDA and yet have highly desirable breeding gain and core performance. The final results of the three phases are intended to establish a reference core design that will be safe, licensable, reliable, and efficient.

#### PROJECT RESULTS

Although not reflected in the work reported, doubling time is not the simple figure of merit that it originally appeared to be. A minimum compound system doubling time is quite desirable when the U.S. utility industry is plutonium limited, i.e., all of the available Pu (owned by the utilities) is being fully utilized in breeder plants. However, this is not the case and probably will not be true until well after the year 2010. Emphasis will be shifted to maximize total net plutonium produced rather than doubling time. In-core inventory will optimize at a somewhat higher quantity of Pu.

As stated in the text there are too many uncertainties in the fuel costs to make them a figure of merit between designs. However, on a consistent basis of estimating, the promising core designs show only small differences in costs. It is highly probable that costs can be significantly improved over those listed in the text.

Edward L. Fuller, Project Manager  
R. K. Winkleblack, Program Manager  
Nuclear Power Division

## ABSTRACT

A parameter study was conducted to determine the interrelated effects of: loosely or tightly coupled fuel regions separated by internal blanket assemblies, number of fuel regions, core height, number and arrangement of internal blanket subassemblies, number and size of fuel pins in a subassembly, etc. The effects of these parameters on sodium void reactivity, Doppler, "incoherence," breeding gain, and thermohydraulics were of prime interest. Trends were established and ground work laid for optimization of a large, radially-heterogeneous, LMFBR core that will have low energetics in an HCDA and will have good thermal and breeding performance.

APPENDIX A: DESIGN ASSUMPTIONS AND CONSTRAINTS

## Table of Contents

	<u>Page</u>
I. General Parameters . . . . .	A-1
II. Fuel Assembly Parameters . . . . .	A-1
III. Blanket Assembly Parameters . . . . .	A-2
IV. Flow Parameter . . . . .	A-2
V. Limiting Conditions . . . . .	A-2
VI. Material Properties . . . . .	A-3
VII. Physics Parameters . . . . .	A-3
VIII. Fuel Management . . . . .	A-5
IX. Economic Parameters . . . . .	A-6
X. Figures of Merit . . . . .	A-6



List of Tables

<u>No.</u>	<u>Title</u>	<u>Page</u>
I.	CRBRP Fuel Assemblies Rod Temperatures Hot Channel/Spot Factors . . .	A-8
II.	Fuel Assembly Plenum Pressure Hot Channel Factors . . . . .	A-11
III.	Radial Blanket Assembly Rod Temperature Hot Channel/Spot Factors . .	A-12
IV.	Radial Blanket Assembly Plenum Pressure Hot Channel Factors . . . .	A-13
V.	Improved 316 Irradiation Induced Swelling - PRLCDS . . . . .	A-14
VI.	Irradiation Induced Creep - PRLCDS . . . . .	A-15
VII.	Improved 316 Stress Rupture - PRLCDS . . . . .	A-16
VIII.	Economic Parameters . . . . .	A-16

## I. General Parameters

A. Reactor Lifetime	30 yrs
B. Net Electric Power	1000 MW
	<p>This value was chosen to allow use of the turbine-generator systems designed during the PLBR studies.</p>
C. Thermal Efficiency	0.32
	<p>This value is defined as the ratio of gross electric power (turbine-generator output) to gross thermal power (reactor power plus pumping heat input).</p>
D. Reactor Inlet Temperature	595 °F
E. Core Temperature Rise	280 °F
F. Cladding and Duct Material	Improved 20% CW316SS
	<p>Material properties are defined in Tables A5-A7.</p>

## II. Fuel Assembly Parameters

A. Spacer Type	Wire
B. Spacer Pitch, inches	12
C. Minimum Cladding Thickness, mils	12
D. Minimum Cladding Thickness-to-o.d. Ratio	0.039
E. Minimum Driver Pin Pitch-to-Diameter Ratio	1.15
F. Nominal Peak Linear Power, kW/ft	15.0
G. Plenum Location	Top
H. Maximum Nominal Subassembly Outlet Temperature, °F	1075 °F
I. Smear Density, % of Theoretical	90.0

### III. Blanket Assembly Parameters

A. Minimum Cladding Thickness, mils	12
B. Minimum Cladding Thickness-to-o.d. Ratio	0.0229
C. Pin Pitch-to-Diameter Ratio	1.07
D. Maximum Smear Density, % of Theoretical	90.0
E. Nominal Peak Linear Power, kW/ft	20.0

### IV. Flow Parameter

A. Hot Channel Factors	Tables Al, 2, 3, 4
B. Maximum Number of Discriminator Zones	15
C. Maximum Pin Bundle Coolant Velocity	35 ft/sec
	This value represents a moderate advance in technology.
D. Maximum Pin Bundle Pressure Drop	90 psi
	Exclusive of entry and exit losses.
E. Bypass Flow	5%
	This fraction of the total flow is un- heated; the remainder is available for cooling driver and blanket assemblies.

### V. Limiting Conditions

A. Fuel Pin Limits	
1. Steady-state and transient CDF	Total steady-state plus transient CDF of 0.75, but neither steady-state CDF nor transient CDF is to exceed 0.50.
2. Cladding temperature for limiting analyses	$2\sigma$ at midwall
B. Duct Limits	
1. Maximum duct-duct interaction	0
	Interaction is measured as distance by which duct wall exceeds pitch line, neglecting axial duct bowing and elastic wall deformation.

2. Maximum Pad Stress

A simplified seismic analysis is to be performed to determine minimum load pad thickness.

3. Maximum Wall Stress  $0.55 \times \sigma_{\text{allowable}}$

Calculated at duct inlet.

4. Bundle-Duct Interaction

Interaction shall be calculated neglecting dispersion and duct creep. The limits stated in this section are to be applied without deviation.

a. 217- and 331-pin bundles  $3 \times \text{wire wrap o.d.}$

b. 169- and 127-pin bundles  $4 \times \text{wire wrap o.d.}$

c. 61- and 91-pin bundles  $5 \times \text{wire wrap o.d.}$

5. Temperature for Interaction Calculations

Bundle-Duct and Duct-Duct Interaction shall be calculated with the entire bundle at the average bundle temperature at each axial position. The duct temperature corresponding to this bundle condition is identical to the average coolant temperature adjacent to the duct wall at each axial position.

VI. Material Properties

Tables A-5, 6, 7

VII. Physics Parameters

A. Heavy Metal Composition

1. Feed Plutonium, % wt	$^{238}\text{Pu}$	0.997
	$^{239}\text{Pu}$	67.272
	$^{240}\text{Pu}$	19.209
	$^{241}\text{Pu}$	10.127
	$^{242}\text{Pu}$	2.395
2. Fertile Uranium, wt %	$^{235}\text{U}$	0.2
	$^{238}\text{U}$	99.8

B. Cross Sections

ENDF/B-IV

### C. Fission Gas Yields

$^{238}\text{U}$ ,  $\text{Pu}$  0.249 atoms/fission

D. Fission Gas Release (%)

90\*

### E. Fission Energy

Use 207 MeV/fission deposited heat  
for all isotopes.

## F. Uncontrolled End-of-Cycle Reactivity

Designs shall conform to an end-of-cycle effective multiplication factor of 1.000 with all control rods withdrawn from the core.

## G. Fluence Limits

Fixed Shield  $2 \times 10^{22}$  nvt  
( $E > 0.1$  MeV)

## H. Controls

## 1. Model

- a. Park controls in upper axial blanket during burn
- b. Use 92% enriched  $B_4C$

## 2. Requirements

- a. Primary system shall be able to maintain shutdown with one withdrawn control rod and the following conditions:

- (1) Hot-to-cold shift
- (2) Reactivity fault
- (3) Excess reactivity at BOEC
- (4) Criticality uncertainty
- (5) Fissile tolerance

b. Secondary system shall be able to maintain shutdown with one withdrawn control rod and the following conditions:

- (1) Hot-to-cold shift
- (2) Reactivity fault

\* Based on LIFE-III analysis.

I. Axial Reflector

1. Composition

Use sod im and steel at core  
volume fractions.

2. Height

to be specified

J. Radial Reflector

1. Composition

a. Fe	$2.16295 \times 10^{-2}$ atoms/ barn-cm
b. Ni	$4.16394 \times 10^{-2}$
c. Cr	$1.39364 \times 10^{-2}$
d. Na	$2.03549 \times 10^{-3}$

2. Thickness

Use a minimum of two rows and add  
whatever thickness is necessary  
for fixed shield fluence limit  
considerations.

VIII. Fuel Management

A. Plant Capacity Factor	70%
B. Refueling Interval	Multiples of 6 months
C. Number of Core Batches	Open
D. Residence Time	
1. Driver Fuel Assemblies	Open
2. Blanket Assemblies	$\leq$ 6 years
E. Number of Enrichment Zones	Open
F. Out-of-Reactor Time	
1. Plutonium Fissile	1.00 years
G. Combined Fabrication/Reprocessing Losses	0.01

## IX. Economic Parameters

A. Fuel Cycle Cost Model	FUCOST, HPC
B. Fabrication Cost Model	HEDL model*
C. Inflation	0%
D. Capital Costs	

Core size effects are to be addressed by the following formula:

$$C_F = 2.4 D + 0.14 DL + 3.2L$$

$C_F$  = Capital cost index (million \$)

D = Diameter of circle which circumscribes removable assemblies (ft)

L = Combined height of core, axial blankets, and fission gas plenum(s) (ft)

## E. Other Parameters

Table A-8.

## X. Figures of Merit

### A. Doubling Time

Calculate individual reactor CSDT for pure cycle reactor using the ANL method.

### B. Breeding Ratio/Breeding Gain

### C. Doppler Coefficient

#### 1. Isothermal Doppler Coefficient

2. Doppler coefficient due to a change in fuel temperature at constant axial, radial, and internal blanket temperature.

### D. Sodium Void Worth

### E. Fuel Cycle Costs

Identify individual components.

---

\*The proposed model is valid for oxide and carbide fuel only.

F. Specific Inventory

Estimate cycle-by-cycle fissile charge  
and discharge for plutonium based on  
equilibrium conditions.

G. Discharge Exposure

Table A - 1  
CRBRP FUEL ASSEMBLIES ROD TEMPERATURES HOT CHANNEL/SPOT FACTORS<sup>(1)</sup>

	<u>Coolant</u>	<u>Film</u>	<u>Cladding</u>	<u>Gap</u>	<u>Fuel</u>	<u>Heat Flux</u>
<u>Direct</u> <sup>(2)</sup>						
Power Level Measurement and Control System Dead Band	1.03					1.03
Inlet Flow Maldistribution	1.05					
Subassembly Flow Maldistribution Calculational Uncertainties	1.08					
Cladding Circumferential Temperature Variation			1.0 <sup>(3)</sup> 1.7 <sup>(4)</sup>		1.0 <sup>(3)</sup>	
<u>Statistical (3<math>\sigma</math>)</u> <sup>(5)</sup>						
Inlet Temperature Variation	1.02 <sup>(6)</sup>	1.0 <sup>(7)</sup>				
Reactor $\Delta T$ Variation	1.04 <sup>(6)</sup>	1.0 <sup>(7)</sup>				
Nuclear Data	1.06					1.065
Fissile Fuel Maldistribution	1.01					1.035

Table A - 1

(Con't)

	<u>Coolant</u>	<u>Film</u>	<u>Cladding</u>	<u>Gap</u>	<u>Fuel</u>	<u>Heat Flux</u>
Wire Wrap Orientation	.1.01					
Subchannel Flow Area	1.028	1.0				
Film Heat Transfer Coefficient		1.12				
Pellet-Cladding Eccentricity		1.15	1.15			
Cladding Thickness and Conductivity			1.12			
Gap Conductance				1.48 <sup>(8)</sup>		
Fuel Conductivity					1.10	
Coolant Properties	1.01					
TOTAL	2 $\sigma$ 1.232 <sup>(6)</sup> 1.221 <sup>(7)</sup>	1.168 1.986 <sup>(4)</sup>	1.128			1.081
	3 $\sigma$ 1.264 <sup>(6)</sup> 1.248 <sup>(7)</sup>	1.234 2.101 <sup>(4)</sup>	1.192	1.48	1.10	1.106

Table A - 1

(Con't)

- (1) Carelli, M.D. and Markley, R.A., "Preliminary Thermal-Hydraulic Design and Predicted Performance of the Clinch River Breeder Reactor Core," ASME Heat Transfer Conference, San Francisco, California, August 11-13, 1975.
- (2) Uncertainties due to physics analysis calculational methods and control rod effects (4% on coolant enthalpy rise) are applied directly on nuclear radial peaking factors.
- (3) For fuel temperature calculations.
- (4) For cladding midwall temperature calculations. Applies to nominal temperature drop between cladding midwall and bulk coolant.
- (5) In addition, the assembly inlet temperature will be increased by 16°F, to account for primary loop temperature control uncertainties.
- (6) Applies to Plant Expected Operating Conditions.
- (7) Applies to Plant T&H Design Conditions.
- (8) Applies to BOL conditions.

TABLE A - 2  
FUEL ASSEMBLY PLENUM PRESSURE HOT CHANNEL FACTORS

		<u>Plenum Temperature</u>	<u>Burnup</u>
<u><b>DIRECT</b></u> <sup>(+)</sup>			
Power Level Measurement		1.02	1.02
Inlet Flow Maldistribution		1.05	
Subassembly Flow Maldistribution			
Calculation Uncertainties		1.08	
<u><b>STATISTICAL (3<math>\sigma</math>)</b></u> <sup>(o)</sup>			
Inlet temperature Variation		1.02 <sup>(ϕ)</sup> 1.0 <sup>(+)</sup>	
Reactor $\Delta T$ Variation		1.04 <sup>(ϕ)</sup> 1.0 <sup>(+)</sup>	
Nuclear Data		1.06	1.06
Fissile Fuel Maldistribution		1.01	1.01
Wire Wrap Orientation		1.01	
Coolant Properties		1.01	
<b>TOTAL</b>	2 $\sigma$	1.216 <sup>(ϕ)</sup> 1.205 <sup>(+)</sup>	1.061
	3 $\sigma$	1.246 <sup>(ϕ)</sup> 1.229 <sup>(+)</sup>	1.082

(+) Uncertainties due to physics analysis calculational methods and control rod effects (4% for both plenum temperature and burnup) are applied directly on nuclear radial peaking factors.

(ϕ) Applies to Plant Expected Operating Conditions.

(+) Applies to Plant T&H Design Conditions.

(o) In addition, the assembly inlet temperature will be increased by 16°F to account for primary loop temperature control uncertainties.

TABLE A - 3

## RADIAL BLANKET ASSEMBLY ROD TEMPERATURE HOT CHANNEL/SPOT FACTORS

	<u>Coolant</u>	<u>Film</u>	<u>Cladding</u>	<u>Gap</u>	<u>Fuel</u>	<u>Heat Flux</u>
<u>DIRECT</u> <sup>(+)</sup>						
Power Level Measurement and Control System Dead Band	1.03					1.03
Inlet Flow Maldistribution	1.07					
Assembly Flow Maldistribution Calculational Uncertainties	1.1	1.05				
Cladding Circumferential Temperature Variation		1.0 <sup>(Δ)</sup> 2.2 <sup>(*)</sup>	1.0 <sup>(Δ)</sup>	1.0 <sup>(Δ)</sup>		
<u>STATISTICAL (3σ)</u> <sup>(o)</sup>						
Inlet Temperature Variation	1.02 <sup>(ϕ)</sup> 1.04 <sup>(ϕ)</sup>	1.0 <sup>(†)</sup> 1.0				
Reactor Δ Variation						
Nuclear Data	1.08					1.09
Fissile Fuel Maldistribution	1.01					1.01
Wire Wrap Orientation	1.01					
- Channel Flow Area	1.035	1.0				
Film Heat Transfer Coefficient		1.21				
Pellet-Cladding Eccentricity		1.15		1.15		
Cladding Thickness & Conductivity				1.12		
Gap Conductance					1.48	
Fuel Conductivity						1.10
Coolant Properties	1.01					
TOTAL	2σ	1.292 <sup>(ϕ)</sup> 1.332 <sup>(ϕ)</sup>	1.284 <sup>(†)</sup> 1.320 <sup>(†)</sup>	1.231 2.708 <sup>(*)</sup> 1.321 2.906 <sup>(*)</sup>	1.128 1.192	1.092 1.10 1.123
	3σ				1.48	

- <sup>(+)</sup> Uncertainties due to physics analysis calculational methods and control rod effects are applied directly on nuclear radial peaking factors. These uncertainty factors are as follows. On coolant enthalpy rise: 1.13 for row 10 at BOC; 1.03 for row 10 at EOC; 1.05 for rows 11 & 12 at BOC; 1.0 for rows 11 & 12 at EOC. On heat flux: 1.19 for row 10 at BOC; 1.08 for row 10 at EOC; 1.10 for rows 11 & 12 at BOC; 1.00 for rows 11 & 12 at EOC.
- <sup>(o)</sup> In addition, the assembly inlet temperature will be increased by 16°F, to account for primary loop temperature control uncertainties.
- <sup>(\*)</sup> For cladding midwall temp. calculations. Applies to nominal temp. drop between cladding midwall and bulk coolant.
- <sup>(Δ)</sup> For fuel temperature calculations.
- <sup>(ϕ)</sup> Applies to Plant Expected Operating Conditions.
- <sup>(†)</sup> Applies to Plant T&H Design Conditions.

TABLE A - 4  
 RADIAL BLANKET ASSEMBLY PLENUM PRESSURE  
 HOT CHANNEL FACTORS

		<u>Plenum Temperature</u>	<u>Burnup</u>
<u><b>DIRECT</b></u>	<u><b>(+)</b></u>		
Power Level Measurement		1.02	1.02
Inlet Flow Maldistribution		1.07	
Assembly Flow Maldistribution			
Calculational Uncertainties		1.10	
<u><b>STATISTICAL (3<math>\sigma</math>)</b></u>	<u><b>(o)</b></u>		
Inlet Temperature Variation		1.02 <sup>(ϕ)</sup> 1.0 <sup>(+)</sup>	
Reactor $\Delta T$ Variation		1.04 <sup>(ϕ)</sup> 1.0 <sup>(+)</sup>	
Nuclear Data		1.08	1.08
Fissile Fuel Maldistribution		1.01	1.01
Wire Wrap Orientation		1.01	
Coolant Properties		1.01	
<b>TOTAL</b>	2 $\sigma$	1.275 <sup>(ϕ)</sup> 1.266 <sup>(+)</sup>	1.075
	3 $\sigma$	1.313 <sup>(ϕ)</sup> 1.299 <sup>(+)</sup>	1.102

(\*) Uncertainties due to physics analysis calculational methods and control rod effects are applied directly on nuclear radial peaking factors. These uncertainties factors (for both plenum temperature and burnup) are as follows: 1.13 for row 10 at BOC; 1.03 for row 10 at EOC; 1.05 for rows 11 & 12 at BOC; 1.0 for rows 11 & 12 at EOC.

(ϕ) Applies to Plant Expected Operating Conditions.

(+) Applies to Plant T&H Design Conditions.

(o) In addition, the assembly inlet temperature will be increased by 16°F to account for primary loop temperature control uncertainties.

Table A - 5

Improved 316 Irradiation Induced Swelling

Stress Free Swelling

$$\text{Swelling} = S = (0.01) R \left[ \phi t + \frac{1}{\alpha} \ln \left\{ \frac{1 + \exp -\alpha(\tau - \phi t)}{1 + \exp (\alpha \tau)} \right\} \right]$$

$$\text{Fractional Volume Change} = \frac{\Delta V}{V_o} = \frac{S}{1-S}$$

$\phi t$  = neutron fluence in units of  $10^{22}$  n/cm<sup>2</sup> (E>0.1 MeV)

$$R(T) = \exp (0.0419 + 1.498\Delta + 0.122\Delta^2 - 0.332\Delta^3 - 0.441\Delta^4) \times 0.7$$

$\Delta = (T - 500)/100$  and T is the temperature in °C

$\alpha = 0.75$

$$\tau_{(\text{nominal})} = 9.0$$

Stress Effect on Swelling

$$\frac{\dot{V}}{V_o} = \left( \frac{\dot{V}}{V_o} \right)_0 \left[ 1 + p \sigma_{\text{HYD}} \right]$$

$\dot{V}/V_o$  = swelling rate

$(\dot{V}/V_o)_0$  = stress-free swelling rate

$\sigma_{\text{HYD}}$  = hydrostatic component of stress, psi

$$p = \left( \frac{T_{\circ F} - 700.0}{100} \right) \times 2 \times 10^{-5} \text{ psi}^{-1}$$

$T_{\circ F}$  = temperature, °F

Table A - 6  
Irradiation Induced Creep

Rate Equation Form

$$\dot{\epsilon}/\bar{\sigma} = \frac{A\phi}{\tau_{tr}} \exp(-\phi t/\tau_{tr}) + DR\phi G(\phi t) + B_o \phi$$

Integrated Form (Constant Stress)

$$\bar{\epsilon}/\bar{\sigma} = A \left[ 1 - \exp(-\phi t/\tau_{tr}) \right] + DR\phi t \left[ 1 - \frac{\Omega}{\phi t} G(\phi t) \right] + B_o \phi t$$

where:  $\bar{\epsilon}$ ,  $\bar{\sigma}$  = effective strain and stress ( $\epsilon$  is fractional and  $\sigma$  has units of psi)

$\dot{\epsilon}$  = effective strain rate ( $\text{sec}^{-1}$ )

$\phi$  = neutron flux,  $\text{n/cm}^2 \text{ sec}$  ( $E > 0.1 \text{ MeV}$ )

$\phi t$  = neutron fluence,  $\text{n/cm}^2$  ( $E > 0.1 \text{ MeV}$ )

$$G(\phi t) = 1 - \exp(-\phi t/\Omega)$$

$$\Omega = 0.753 \tau \left( \text{n/cm}^2, E > 0.1 \text{ MeV} \right)$$

$$R(T) = \exp (0.0419 + 1.498\Delta + 0.122\Delta^2 - 0.332\Delta^3 - 0.441\Delta^4) \times 10^{-22} \times 0.7$$

$$\Delta = (T - 500)/100 \text{ and } T \text{ is the temperature in } {}^\circ\text{C}$$

$$B_o = 3 \times 10^{-30} \text{ psi}^{-1} \text{ n}^{-1} \text{ cm}^2$$

$$\tau_{(\text{nominal})} = 9.0 \times 10^{22} \text{ n/cm}^2$$

$$D = 2 \times 10^{-5} \text{ psi}^{-1}$$

$$A = 1 \times 10^{-8} \text{ psi}^{-1}$$

$$\tau_{tr} = 0.2 \times 10^{22} \text{ n/cm}^2$$

Table A - 7  
Improved 316 Stress Rupture

$$\log_{10} t_r = -15.2420 + 18910.4/T_{\circ K} + 7.39226 \log_{10} \left( \log_{10} (90/\sigma_{ksi}) \right)$$

where:  $t_r$  = time to rupture, hours  
 $T_{\circ K}$  = temperature,  $^{\circ}$ K  
 $\sigma_{ksi}$  = rupture stress, ksi

Table A - 8  
Economic Parameters

Year for Constant Dollars	1977
Plant Lifetime	30 years
Planning Horizon for Fuel Cycle Optimization	30 years
Cost of Money	7.5%/yr*
Fraction of Investment in Debt	0.50
Cost of Debt	5.0%/yr
Cost of Equity	10.0%/yr
Fabrication Costs	HEDL model
Reprocessing Costs	\$350/kg HM
Plutonium Value	100 \$/gm
Uranium-233 Value	80 \$/gm
Spent Fuel Shipping Costs	\$80/kg HM
Waste Shipping Costs	\$50/kg HM
Waste Storage Costs	\$115/kg HM

\*Real, i.e., deflated cost

APPENDIX B: RADIALLY HETEROGENEOUS CORE CONFIGURATIONS

## Table of Contents

	<u>Page</u>
1.0 INTRODUCTION . . . . .	B-1
2.0 PROBLEM DEFINITION . . . . .	B-3
3.0 APPROACH . . . . .	B-5
4.0 LOW SODIUM VOID CORES . . . . .	B-7
4.1 Loosely Coupled Cores . . . . .	B-7
4.1.1 Center Blanket Configurations . . . . .	B-7
4.1.2 Center Core Configurations . . . . .	B-9
4.1.3 Core Height Reduction . . . . .	B-11
4.1.3.1 Fixed Configuration . . . . .	B-12
4.1.3.2 Change in Region Size . . . . .	B-13
4.1.3.3 Change in Region Number . . . . .	B-14
4.1.4 Depletion Analysis . . . . .	B-14
4.1.5 Intercomparison . . . . .	B-14
4.1.5.1 Center-Blanket 2-Core vs. 3-Core Zone Configurations . . . . .	B-14
4.1.5.2 Central Blanket 3-Core Zone vs. Center Core 3-Core Zone Configurations . . . . .	B-16
4.1.6 Sensitivity Analysis . . . . .	B-17
4.1.6.1 Volume Split . . . . .	B-18
4.1.6.2 Enrichment Split . . . . .	B-18
4.2 Tightly Coupled Cores . . . . .	B-18
4.2.1 Center Blanket Configurations . . . . .	B-19
4.2.2 Center Core Configurations . . . . .	B-20
4.2.3 Core Height Variation . . . . .	B-20
4.2.4 Depletion Analysis Results . . . . .	B-21
4.2.5 Intercomparison . . . . .	B-22
4.2.6 Sensitivity Analysis . . . . .	B-23
4.2.6.1 Enrichment Split . . . . .	B-23
5.0 CONCLUSIONS . . . . .	B-25
6.0 ACHIEVABLE SODIUM VOID REACTIVITIES . . . . .	B-27



### List of Figures

<u>No.</u>	<u>Title</u>	<u>Page</u>
1.	Effect of Core Layout on Sodium Void Reactivity . . . . .	B-28
2.	Low Sodium Void Cores . . . . .	B-28
3.	Loosely Coupled Center Blanket Cores . . . . .	B-29
4.	Loosely Coupled Center-Core Cores . . . . .	B-29
5.	Tightly Coupled Center-Blanket Cores . . . . .	B-30
6.	Tightly Coupled Center-Core Cores . . . . .	B-30
7.	Loosely-Coupled, Center-Blanket, Two Core Zones . . . . .	B-31
8.	Loosely-Coupled, Center-Blanket, Three Core Zones . . . . .	B-32
9.	Loosely-Coupled, Center-Core, Three Core Zones . . . . .	B-33
10.	Configuration for Core Height Reduction Evaluations . . . . .	B-34
11.	Sodium Void Reactivity as a Function of Core Height . . . . .	B-34
12.	Configurations for Three Different Core Heights (271 Pins per Assembly) . . . . .	B-35
13.	Configuration for 22.53 in. High Core (271 Pins per Assembly) . . . . .	B-36
14.	Loosely-Coupled Configurations for Burnup Calculations . . . . .	B-37
15.	Sodium Void Reactivity as a Function of Core Volume Split . . . . .	B-38
16.	Tightly Coupled Center Blanket Cores . . . . .	B-39
17.	Tightly Coupled Center-Core Cores . . . . .	B-40
18.	Core Configurations for Depletion Analysis . . . . .	B-41



List of Tables

<u>No.</u>	<u>Title</u>	<u>Page</u>
I.	Loosely-Coupled, Center Blanket, Two Core Zones . . . . .	B-42
II.	Loosely-Coupled, Center Blanket Three Core Zones . . . . .	B-43
III.	Loosely-Coupled Center-Core, Three Core Zones . . . . .	B-44
IV.	Effects of Core Height Reduction on Sodium Void Reactivity . . . . .	B-44
V.	Loosely-Coupled, Center-Blanket, Two Core Zones . . . . .	B-45
VI.	Loosely-Coupled, Center-Blanket, Three Core Zones . . . . .	B-46
VII.	Loosely-Coupled, Center-Core, Three Core Zones . . . . .	B-47
VIII.	Loosely Coupled Cores, Power Peaking Sensitivity on Enrichment Changes . . . . .	B-48
IX.	Center Blanket Tightly Coupled Cores . . . . .	B-49
X.	Tightly Coupled Center Core Configurations . . . . .	B-50
XI.	Core Height Variation of a Tightly Coupled Center Core Configuration . . . . .	B-51
XII.	Core Height Variation with a Change in the Number of Core Zones . .	B-52
XIII.	Tightly Coupled Core Intercomparison . . . . .	B-53
XIV.	Tightly Coupled Core Intercomparison . . . . .	B-54
XV.	Tightly Coupled Cores Power Peaking Sensitivity to Enrichment Changes . . . . .	B-55
XVI.	Achievable Sodium Void Reactivities (Two-Year Residence Time, Multi-Batch Refueling) . . . . .	B-55
XVII.	Loosely Coupled Cores . . . . .	B-56
XVIII.	Tightly Coupled Cores . . . . .	B-56

## 1.0 INTRODUCTION

It is well known that the heterogeneous core concept can be an effective means for reducing the sodium void reactivity of a large LMFBR core. This reduction results, in principle, from an increase in the neutron leakage, with respect to a homogeneous core, due to the placement of blanket assemblies or blanket regions into the fuel region. It is obvious that the number of different possible heterogeneous core configurations is very great and that not all can be investigated. Thus, as a first step in the optimization and design studies, we have attempted to narrow the options by an analysis of the generic possibilities and limitations of the heterogeneous core concept solely with respect to achieving a low sodium void reactivity.

The two types of heterogeneity commonly considered are the radially heterogeneous configuration and the axially heterogeneous configuration. The latter concept has already been shown not to be viable. We, therefore, consider only the radially heterogeneous concept.



## 2.0 PROBLEM DEFINITION

At first glance it would appear that the reduction in sodium void reactivity is proportional to the number of internal blankets in the fuel region. This is true to some extent. However, as Fig. 1 shows, the sodium void reactivity is also strongly dependent on the arrangement of the internal blankets in the core. In Fig. 1 we have two cores with the same number of fuel assemblies and the same number of internal blanket assemblies, yet the sodium void reactivities of these two cores differ by a factor of two. Clearly, the particular configuration of fuel and blanket assemblies can play a dominant role in the reduction of the sodium void reactivity. The above example and the general approach of increasing the leakage surface of the core indicate that the sodium void reactivity of a heterogeneous core will decrease as the individual core regions get smaller and are more neutronically decoupled. However, as we pursue low sodium void configurations some general design constraints, such as the control required per region, the peak power swing in a core region over a burn cycle, the peak power sensitivity in one region due to enrichment changes in another region, and a reasonable reactor diameter, eliminate a large number of theoretically possible configurations. This phase of the study addresses the problem of determining low sodium void configurations ( $< \$2.50$  at the EOC) which have a system doubling of approximately 15 years and meet basic LMFBR design constraints.



### 3.0 APPROACH

Previous studies have shown that the detailed design of the fuel and blanket assemblies does not have a great impact on the sodium void reactivity of a given heterogeneous configuration for as long as the fuel volume fractions in fuel and blanket assemblies are in the 40% and 55% range, respectively. In this screening phase of the study, we have, therefore, used the same assembly designs for the fuel and blankets as in the Phase 'A' core. The assembly size, however, was changed as the number of fuel pins per assembly changed. In addition we have found that over a wide range of heterogeneous core configurations the increase in the sodium void reactivity from BOL to EOEC is roughly \$1.00. Thus, for simplicity, the initial screening was done for BOL conditions even though the EOEC sodium void reactivity will be the design limiting sodium void reactivity.

The approach in this study consisted in essence of rearrangement of internal blanket assemblies in the core, a change in the number of internal blankets, a change in the neutronic coupling between core zones, and a change in the core height. In Figs. 2 through 6 schematic outlines of some of the options available for reducing the sodium void reactivity are given. A broad division of the low sodium void cores into two classes is made in Fig. 2. These are the tightly coupled and the loosely coupled cores. Although these two terms are not very precise, we have found them useful. Generally speaking, tightly coupled means that the fuel regions are separated by roughly one row of blanket assemblies, and loosely coupled means that about two rows of blanket assemblies separate the fuel regions. Each of these two classes can now be further divided into cores with a center blanket region and cores with a center fuel region.

Within each of these classes there are many available options which can lead to a reduction in the sodium void reactivity. These are outlined in Figs. 3 through 6. For tightly or loosely coupled cores we have a choice in the number of fuel regions, the degree of neutronic coupling between fuel regions, the size of the center blanket or center core region, and a choice

in the core height. In the last case, there are additional options as to how the reactor power is conserved as the core height is reduced. The full range of these options was not investigated in each class since their effect is expected to be about the same in many cases.

To facilitate the discussion of the different configurations we use the following symbolic nomenclature. The two main divisions, the loosely coupled and the tightly coupled cores are abbreviated LC and TC, respectively. Within these categories we have configurations with a center balnket (CB) or a center core (CC). In addition a distinction is made as to the number of core zones (2C, 3C, 4C, etc.) and between similar configurations with respect to the above classification. For example, CB-2C-3 is a center blanket two core zone configuration. The number 3 indicates that it is the third configuration within this category. The distinction between LC and TC will be stated separately.

## 4.0 LOW SODIUM VOID CORES

### 4.1 LOOSELY COUPLED CORES

In this section we consider the class of configurations where the fuel zones are separated by roughly two rows of blanket assemblies. We could, of course, separate the fuel zones by thicker internal blanket regions and decouple the fuel regions even more. However, previous studies have shown that by increasing the internal blanket thickness to more than two rows, little is gained with respect to sodium void reduction while the problems of peak power sensitivity with respect to variations in enrichment and control are greatly exacerbated.

#### 4.1.1 Center Blanket Configurations

In this analysis we look at three core configurations each with a central blanket region and two core regions. The configurations are shown in Fig. 7. The common element in these three configurations is the total number of fuel assemblies 354 and that the core regions are separated by two rows of internal blanket assemblies in each case. The three configurations differ in the size of the central blanket and the total number of internal blanket assemblies. A more detailed description of the similarities and differences of these configurations is given in Table I.

The sodium void reactivities for these configurations are also given in Table I. We see that as the size of the center blanket region is increased from 31 to 55 and then to 91 assemblies (this also increases the total number of internal blankets) the core sodium void reactivity decreases by about 25% in each case. This decrease is evident not only for the total core values but also for each of the core regions. This trend in the sodium void reactivity can be attributed to the reduction in the effective core region thickness as the central blanket is increased from 31 assemblies to 55 and then to 91. The inner core effective region thickness decreases by about 10% in each case and that of the outer core region by about 8% in each case. On the other hand, the effective region thickness of the internal blanket separating the core regions increases by only 3 and 1%, respectively, since the region is fixed to two rows of assemblies.

The increase in the size of the center blanket leads to a larger fuel region surface. The decrease in the effective thickness of the fuel regions leads to an increase in the flux gradient. Both effects contribute to an increase in the leakage into the blankets and consequently to a decrease in the sodium void reactivity. The increase in the effective thickness of the internal blanket region separating the two core zones tends to decouple the core zones. This also lowers the sodium void reactivity, but because the increase in the effective thickness of this blanket region is relatively small, from 3 to 1%, its contribution to the decrease in sodium void reactivity in these cases is also relatively small.

Thus, for a center blanket configuration at a fixed power, increasing the center blanket decreases the sodium void reactivity of the core. The basic reason for this is, however, the consequent decrease in the effective thickness of the fuel regions.

This approach of making the effective thickness of the core zones smaller, yet maintaining the same total power (354 assemblies as above) can also be achieved by increasing the number of fuel zones to three and increasing the number of blanket assemblies separating the core zones rather than increasing the number of central blanket assemblies. The configurations shown in Fig. 8 result from such an approach. Here we consider three cores each with a central blanket and three fuel regions. The central blanket is fixed to 13 assemblies. The number of fuel assemblies in the inner, middle, and outer cores are 54, 102, and 198, respectively for each configuration. The pertinent descriptive data and the sodium void reactivities for these cores are given in Table II. The variable in each case is the number of blanket assemblies separating the core zones. For example, configuration CB-3C-1 has 12 more internal blanket assemblies in the internal blanket region separating the inner core from the middle core than CB-3C-2, while CB-3C-2 has 12 more blanket assemblies in the internal blanket separating the middle core from the outer core than configuration CB-3C-3. Thus, the dominant contribution to a change in the sodium void reactivity will come from the change in the neutronic coupling between the core regions due to a change in the effective thickness of the internal blankets. The effective thickness of the core regions changes very little (up to 3%) due to the changes in the internal blanket thickness, and thus is not the issue in these cores. On the other hand, the effective thickness of the internal blanket separating the inner core from the middle core is about 15% lower in configuration CB-3C-2

than in CB-3C-1. The increased coupling between these core regions is reflected in the increase of the sodium reactivity in configuration CB-3C-2 for these regions. The inner core sodium void reactivity increases by 38% while that of the middle core increases by 18%. The relative change in the outer core is insignificant. The total core sodium void reactivity increases by about 18%.

In configuration CB-3C-3 the effective thickness of the internal blanket separating the middle core from the outer core has been decreased by about 9% from that of configuration CB-3C-2. This increased neutronic coupling is again reflected in the sodium void reactivity of the configurations. The coupling between the inner core and the middle core has not been changed in this case, and consequently, the change in sodium void reactivity for the inner core is relatively insignificant. But the sodium void reactivity of the middle core increases by 17.4% and that of the outer core by 40%. The total core sodium void reactivity is 16.5% higher for CB-3C-3 than for CB-3C-2.

We note that with respect to these six loosely coupled center blanket heterogeneous configurations nearly the same low sodium void reactivity can be achieved by either a two core zone configuration (0.218%  $\Delta k$ ) or by a three core zone configuration (0.220%  $\Delta k$ ). Further reductions could be achieved but at the expense of other performance parameters.

#### 4.1.2 Center Core Configurations

The other class of radially heterogeneous cores that we consider have configurations with a center core region. In principle we could construct a two core zone configuration with a center core. This, however, based on the study of the center blanket configurations, would lead to a core with a sodium void reactivity greater than that for a center blanket configuration. Since in the latter the core surface will be greater and the core regions relatively thinner. In a three core zone configuration this conclusion is no longer evident, since in the construction of such configurations there is far more leeway in choosing the appropriate amount of decoupling and the best effective thickness of the core zones.

For the generic study four different core configurations were chosen each with three core zones. The core layouts are given in Fig. 9. The common element in these configurations is the total number of fuel assemblies which is fixed at 360. The number of internal blanket assemblies is varied and different proportions of fuel assemblies between the three core regions are considered. Further details are given in Table III.

Configuration CC-3C-1 exhibits the highest total core sodium void reactivity of  $0.302\% \Delta k$ . The largest contribution comes from the middle core zone where the sodium void reactivity ( $0.162\% \Delta k$ ) is about twice as great as that of the next largest contribution  $0.082\% \Delta k$  from the outer core zone. Experience in the construction of low sodium void cores has shown that for reasonable configurations the marginal increase in the sodium void reactivity per fuel assembly is least for the outer core zone. Thus, to reduce the sodium void reactivity of this core, we construct configuration CC-3C-2 by taking six fuel assemblies out of the inner core, twelve fuel assemblies out of the middle core, and placing them into the outer core. In addition, we decrease the neutronic coupling between the inner and middle cores by increasing the number of blanket assemblies from 48 to 54 in the internal blanket region between these core zones. These changes have the expected results on the sodium void reactivity. In the inner core zone the sodium void reactivity is reduced by 55%, in the middle core zone by 31% and in the outer core zone, where we have added the fuel assemblies, it increases by 52%. The total core sodium void reactivity of  $0.262\% \Delta k$  is about 13% lower.

In configuration CC-3C-2 the contributions from the individual core zones are distributed such that the greatest contribution,  $0.125\% \Delta k$ , comes from the outermost core zone, almost as much,  $0.111\% \Delta k$ , from the middle core zone, and less than a quarter of either,  $0.026\% \Delta k$ , from the center core zone. The sodium void reactivity of this core can be further reduced by constructing configuration CC-3C-3. Here fuel assemblies have been removed from the outer core zone (the highest contribution) to the center core zone (the lowest contribution). But since the marginal increase in the sodium void reactivity due to the addition of a fuel assembly is greater in the center core zone than the marginal decrease in the outer core zone, we must also decrease the neutronic coupling between the inner and the middle core zones. The latter is achieved by increasing the number of internal blanket assemblies from 54 to 66 in the blanket region between these core zones. In addition, by increasing the number of internal blanket assemblies from 114 to 126 in the blanket region separating the middle and outer core zones, we further reduce the sodium void reactivity by decreasing the neutronic coupling also between these core zones. The resultant total core sodium void reactivity of configuration CC-3C-3 is 11% less than that of CC-3C-2. The skew in the distribution of the sodium void reactivity contributions has been reversed, so that now the center core zone gives the highest contribution and the outer core zone the lowest.

The core zones in configuration CC-3C-3 are each separated by two rows of internal blankets. This we feel is about the maximum thickness, for further decoupling would lead to extreme sensitivities with respect to power peaking between the individual core regions. Thus, to further reduce the sodium void reactivity, we can again redistribute the fuel assemblies between the core zones. We arrive at configuration CC-3C-4, by removing 12 fuel assemblies from the center core (where the marginal change in the sodium void reactivity due to a fuel assembly is highest) and placing them into the middle core region (where the marginal change in the sodium void reactivity due to a fuel assembly is less). This has the effect of reducing the sodium void reactivity of the inner core more than the increase in the sodium void reactivity of the middle core. The outer core zone is not significantly affected. Thus the total core sodium void reactivity is reduced from 0.232%  $\Delta k$  to 0.208%  $\Delta k$ .

It would appear, therefore, that we could continue with this approach and reduce the sodium void reactivity even further. For example, by taking fuel assemblies from the middle core zone and placing them into the outer core zone. This would probably have the desired effect. But we must keep in mind that we are not seeking a core with the lowest possible sodium void reactivity, and that there are many other constraints, such as breeding performance, power distribution, and behavior during burnup, which have not been taken into account and will ultimately have a major impact on the core selection.

#### 4.1.3 Core Height Reduction

One option for lowering the sodium void reactivity is to increase the leakage through a core height reduction. However, a heterogeneous core is already "leaky" due to the large radial leakage into the internal blankets. The question, therefore, is whether in the case of a heterogeneous core a significant reduction in the sodium void reactivity can be achieved through a core height reduction. Or, on the other hand, how much is lost with respect to sodium void reactivity by increasing the core height should this become expedient because of some other considerations.

When the core height in a heterogeneous reactor is changed, the reactor power can be conserved in three different ways. One is to vary the number of fuel pins per assembly and essentially maintain the same core layout. The other is to vary the number of assemblies per core region while keeping the number of fuel pins per assembly fixed. In the latter case, care must be taken as to where the additional assemblies are placed, for their worth will differ for different core regions. The third option is to change the number of fuel assemblies by changing the number of core regions.

#### 4.1.3.1 Fixed Configuration

To determine the effect of the core height reduction for a fixed configuration, the following generic comparison was made. In one case, the core height was varied without normalization of the reactor power, while in the other case, the core height was varied and the power output was kept constant by changing the number of fuel pins per assembly. As the number of fuel pins per assembly was changed, the assembly size was changed accordingly. The core chosen for this analysis was a center blanket two core zone configuration. The core layout is given in Fig. 10. At a core height of 41.73 in., this configuration with 271 pins per fuel assembly has a total core sodium void reactivity of 0.310%  $\Delta k$ . In Fig. 11 the dashed line represents the variation of the sodium void reactivity with respect to a change in core height without normalization of the power. The solid line, on the other hand, represents the change in the sodium void reactivity due to a core height variation, but where the total power output has been normalized by changing the number of pins per assembly. The dashed line is above the solid curve for core heights greater than 41.73 in. since these cores are physically larger systems than the reference core. For core heights less than 41.73 in. the opposite is true.

It would appear from the trend exhibited by these curves that the dominant contribution to the reduction of the sodium void reactivity comes from the reduction of the core height. A closer examination, however, shows that other effects, which are specific to this method of conserving the power with respect to core height reduction, also contribute to a reduction in the sodium void reactivity. These effects are a consequence of the fact that as we increase the number of fuel pins per assembly in these calculations we also increase the assembly size proportionally. This increases the effective thickness of the fuel and blanket regions. Qualitatively we can explain these effects in the following way. In the case of a fuel region, core height reduction decreases the surface area which is perpendicular to the radial direction. In addition, the increase in the radial dimension of the region results in some flux flattening. Both lead to a decrease in the radial leakage and an increase in the sodium void reactivity. While in the axial direction, core height reduction leads to an increase in the neutron leakage and the axial flux gradient which results in a reduction of the sodium void reactivity.

Due to the larger size of the fuel assembly, the blanket assembly has increased by the same amount. This results in an increase in the effective

thickness of the center blanket and of the blanket region separating the inner and outer core regions. The former effect increases the radial surface area of the fuel regions and reduces somewhat their effective thickness. The latter effect decreases the neutronic coupling between the fuel regions. Both result in a reduction of the sodium void reactivity. Thus the reduction in the sodium void reactivity that we see in Fig. 11, for the cores where the power has been normalized, is more the consequence of an increase in the blanket thickness than in the reduction of the core height.

#### 4.1.3.2 Change in Region Size

The other method of normalizing the power when the core height is changed is to increase the number of fuel assemblies in the core region rather than the number of pins per assembly. This approach does not affect the size of the internal blanket assemblies and thus the attendant changes in the sodium void reactivity are mostly eliminated.

The core layouts for this analysis are given in Fig. 12. The core height is varied from 33.5 in. to 48 in. The reference core at 41.73 in. is the same as in the previous cases where the number of fuel pins per assembly had been changed. The sodium void reactivities for these configurations are given in Table IV. The reference configuration has 366 fuel assemblies of which 114 are in the inner core and 252 are in the outer core. As we reduce the core height of the reference core to 33.5 in., 18 fuel assemblies are added to the inner core and 72 to the outer core, to maintain the same power. The internal blanket between the inner and outer core regions is kept at two rows. Thus roughly the same neutronic coupling is maintained.

The sodium void reactivity is reduced by about 4% with this approach, while previously the reduction was about 40%. (The reduced core heights are slightly different, 33.5 in. in this case as compared to 34.16 in. in the previous case. However, this will not affect the conclusions of the comparison.) Similar differences in the increase in the sodium void reactivity as the core height is increased are also evident. These results, therefore, illustrate that in the case of core height reduction in a heterogeneous core, it is important to keep in mind what phenomena are the causes for the reduction in the sodium void reactivity. For different methods of normalizing the power as core height is decreased lead to different degrees of sodium void reduction.

#### 4.1.3.3 Change in Region Number

The third approach to normalizing the power as the core height is reduced is to add another core region. This case is shown in Fig. 13. The configuration was constructed by taking the reference configuration Fig. 10 and adding a third core zone, which consists of three rows of fuel and is separated from the neighboring core zone by two rows of internal blankets. The core height must then be reduced to 22.5 in. to maintain the same power. The resultant configuration then has a sodium void reactivity of  $-0.151\% \Delta k$ . This is because we have almost doubled the core surface area and, therefore, greatly enhanced the negative leakage component of the sodium void reactivity. The disadvantage of this type of approach is that the core diameter has been increased to about 21 ft from the former 16 ft.

#### 4.1.4 Depletion Analysis Results

Although the safety characteristics of an LMFBR, as expressed by its sodium void reactivity, are extremely important constraints, of no less significance is the LMFBR's breeding and thermal performance. That is, in addition to being safe, the reactor must also be economically viable. One criterion for the latter is the reactor's breeding performance. Therefore, we now take the selection process one step further and analyze some of the previous configurations, especially those with BOL core sodium void reactivities less than  $\$2$ , with respect to their breeding and burnup characteristics during an equilibrium cycle.

#### 4.1.5 Intercomparison

##### 4.1.5.1 Center-Blanket 2-Core vs. 3-Core Zone Configurations

The loosely-coupled configurations which have been selected for burnup analysis are shown in Fig. 14. The top two configurations, CB-2C-2 and CB-2C-3, are center blanket two core configurations. The middle two, CB-3C-1 and CB-3C-3, are center blanket three core configurations, while the bottom two, CC-3C-2 and CC-3C-3, are center core three core configurations. The burnup analysis was performed for equilibrium cycle conditions with annual refueling, a two year residence time for the core and internal blanket assemblies, and a five year residence time for the radial blanket assemblies. The analysis was done for two core heights (41.73 in. and 34.16 in.) with the power conserved through an increase in the number of fuel pins per assembly from 271 to 331. The lower core heights were included to insure that low sodium void reactivity

cores can be derived since the sodium void reactivity at the EOEC was expected to be at least \$1 greater than at BOL. This increase in the sodium void reactivity could best be mitigated by using, in conjunction with a core height reduction, the approach of increasing the number of fuel pins per assembly.

In Table V, we compare two center-blanket two core zone configurations at two core heights. The two configurations, CB-2C-2 and CB-3C-3, differ in the total number of internal blankets. In the first configuration there are 169 blanket assemblies of which 55 are in the center blanket region. In the second configuration there are 217 of which 91 are in the center blanket region.

These two configurations, at a core height of 41.73 in., have comparable reactor doubling times, 15.4 years for the former and 15.6 for the latter. As we decrease the core height to 34.16 in. these increase somewhat to 15.9 and 16.1 years, respectively.

The sodium void reactivity for configuration CB-2C-2 at the 41.73 in. core height increases from 0.238%  $\Delta k$  at BOL to 0.672%  $\Delta k$  at EOEC when the flowing sodium is voided from the core and upper axial blankets. Similarly, for configuration CB-2C-3 this change is from 0.169%  $\Delta k$  at BOL to 0.579%  $\Delta k$  at EOEC. Lowering the core height to 34.16 in. reduces the EOEC sodium void reactivity to 0.497%  $\Delta k$  in configuration CB-2C-2 and 0.409%  $\Delta k$  for configuration CB-2C-3. The burnup swings for these two configurations are nearly equal, 0.0210  $\Delta k$  for configuration CB-2C-2 and 0.0214  $\Delta k$  for configuration CB-2C-3. For the lower core height the swing of the former increases to 0.0269  $\Delta k$ . In the case of the latter, configuration CB-2C-3, the swing increases to 0.0270  $\Delta k$  as the EOEC fissile inventory increases from 5235 kg to 5352 kg.

The results for the center-blanket three core zone configurations, CB-3C-1 and CB-3C-3, are given in Table VI. The total number of fuel assemblies in these two configurations is 354, as in configurations CB-2C-2 and CB-2C-3 which were discussed above. The total number of internal blanket assemblies is 205 in configuration CB-3C-1 and 181 in CB-3C-3. We again consider two core heights, 41.73 in. and 34.16 in., and maintain a constant power by changing the number of fuel pins per assembly from 271 to 331 as the core height is reduced.

In both configurations the number of fuel assemblies per core region is the same 54/102/198. The center blanket regions are also the same with 13 internal blanket assemblies. The configurations differ in the number of

internal blanket assemblies which separate the core zones. Configuration CB-3C-1 has 72 internal blanket assemblies separating the first core zone from the second, and 120 internal blanket assemblies between the second core zone and the third. On the other hand, configuration CB-3C-3 has 60 internal blanket assemblies between the first core zone and the second and 108 between the second and third. Thus, core zone one and two are more decoupled in CB-3C-1 than in CB-3C-3, while core zone two and three are more decoupled in CB-3C-3 than in CB-3C-1.

The sodium void reactivities (for voiding the core and the upper axial blanket of flowing sodium at the EOEC), at a 41.73 in. core height, are 0.576%  $\Delta k$  for configuration CB-3C-1 and 0.671%  $\Delta k$  for configuration CB-3C-3, and at a 34.16 in. core height, 0.381%  $\Delta k$  and 0.475%  $\Delta k$ , respectively. The lower sodium void reactivity for configuration CB-3C-1, shows that changes in the effective thickness of the internal blanket between core zone one and two affect the sodium void reactivity far more than changes in the effective thickness of the internal blanket between core zone two and core zone three.

The reactor doubling times for these two configurations are comparable, 15.8 years for CB-3C-1 and 15.4 years for CB-3C-3, at a core height of 41.73 in. For the shorter cores, the respective reactor doubling times increase to 16.3 years and 15.9 years.

We can compare the performance parameters between the two types of configurations, center blanket two core zone and center blanket three core zone, by looking at two representative configurations. If we take, for example, CB-2C-2 and CB-3C-3 at a core height of 41.73 in., we see that with respect to reactor doubling time and sodium void reactivity they do not differ. The reactor doubling time is 15.4 years for each and the sodium void reactivities are 0.672%  $\Delta k$  and 0.671%  $\Delta k$ , respectively. The differences between these two configurations in the BOEC fissile inventories and the burnup swings are significantly greater. For the center blanket two core zone configuration the BOEC fissile inventory is 4995 kg and the burnup swing 0.0210  $\Delta k$ , while for the center blanket three core zone configuration these values are 5352 kg and 0.0083  $\Delta k$ . In choosing between different LMFBR designs, it is desirable to have both a low fissile inventory and a low burnup swing. On this basis a clear cut choice between the two configurations cannot be made.

#### 4.1.5.2 Central Blanket 3-Core Zone vs. Center Core 3-Core Zone Configurations

The two center core configurations considered for depletion analysis are CC-3C-2 and CC-3C-3 shown in Fig. 14. Again, two core heights are considered

and the power is conserved by changing the number of fuel pins per assembly. The total number of fuel assemblies is 360 which are divided into three core zones as 30/108/222 for configuration CC-3C-2 and 42/120/198 for configuration CC-3C-3. The number of internal blankets separating these core zones are 54/114 for configuration CC-3C-2 and 66/126 for CC-3C-3. Although the total number of internal blankets is quite different in these two configurations, we note from Fig. 14 that the internal blankets are all two rows thick. Thus, the effective coupling between the core regions should be roughly the same, and any differences in performance can be attributed to differences in the distribution of core assemblies.

The reactor doubling times at a core height of 41.73 in. are given in Table VII, and are 15.1 years for configuration CC-3C-2 and 15.6 years for CC-3C-3. At a core height of 34.16 in. we get 15.7 and 16.1 years, respectively. The burnup swings for these two configurations are nearly the same 0.0147  $\Delta k$  for CC-3C-2 and 0.0150  $\Delta k$  for CC-3C-3 at a core height of 41.73 in. and for a 34.16 in. core, 0.0219  $\Delta k$  and 0.0223  $\Delta k$ , respectively. The sodium void reactivities for these two configurations, with tall cores, are 0.661%  $\Delta k$  and 0.596%  $\Delta k$  for CC-3C-2 and CC-3C-3, respectively, and similarly 0.465%  $\Delta k$  and 0.401%  $\Delta k$  for the short cores.

In comparing the performance of the center-blanket three core zone configurations (Table VI) and the center core three core configurations (Table VII), it is evident that with respect to these data neither type of configuration is clearly superior. The reactor doubling times are all in the neighborhood of 15 to 16 years and the EOC sodium void reactivities for voiding the flowing sodium in the core and the upper axial blanket are between \$1.65 and \$2.00 for the tall cores, and 30 to 35% less for the short cores.

#### 4.1.6 Sensitivity Analysis

In the previous sections it was seen that for a given number of core zones in a radially heterogeneous core the distribution of fuel assemblies between the core zones affects the sodium void reactivity. In addition, since a heterogeneous core is effectively composed of a number of small coupled reactors, it is also of interest to determine the power peaking sensitivity with respect to enrichment split.

#### 4.1.6.1 Volume Split

In order to examine the sensitivity of the sodium void reactivity to volume split, we take a two core zone configuration. This configuration consists of 354 fuel assemblies, a center blanket of 55 assemblies, and two rows of internal blankets separating the core zones. In Fig. 15 the sensitivity of the sodium void reactivities for the inner and outer core zones and the total core are given as a function of the inner to total core volume ratio. We note that in the range of 0.25 to 0.40 for the ratio of inner to total core volume the sodium void reactivity varies by less than 3%. Although larger variations in this ratio were not explicitly calculated, it is evident on heuristic grounds that outside this range, as we tend toward a single large homogeneous reactor, the sodium void reactivity of the system will increase substantially. Nevertheless, regimes do exist where there is some room for interchanging a few fuel assemblies between core zones without significantly effecting the sodium void reactivity.

#### 4.1.6.2 Enrichment Split

In a heterogeneous core the different core zones can be considered to some extent as a collection of coupled subcritical cores. Due to the neutronic coupling between these cores a change in the enrichment of one region will affect the power peaks in the other regions. In Table VIII the power peaking sensitivity of the innermost core zone is given due to 0.5% changes in the enrichment of the innermost, and outermost core zone. The change in the peak power densities in the inner core zone is about the same for the center blanket configurations, a little over 5%. The center core configuration has a somewhat greater sensitivity, the power density in the inner core changes by 7% while that of the outer core by 8.2%.

### 4.2 TIGHTLY COUPLED CORES

In this section we consider the class of configurations where the fuel zones are separated by roughly one row of internal blanket assemblies. The analysis is along the same lines as in the case of the loosely coupled cores. We again consider center blanket and center core configurations with different numbers of core zones. In addition, the effect of core height variation on the sodium void reactivity is also investigated.

#### 4.2.1 Center Blanket Configurations

The six tightly coupled center blanket configurations considered in this study are shown in Fig. 16. There are one configuration with two core zones CB-2C-6, three configurations with three core zones CB-3C-1, CB-3C-2, CB-3C-3, one configuration with four core zones CB-4-4, and one with six core zones CB-6C-5. The common element in all these configurations is that the total number of fuel assemblies is fixed at 354. The detailed information with respect to the number of fuel and blanket assemblies per region, sodium void reactivity, and the fissile inventory are given in Table IX.

In addition to having the same number of fuel assemblies, configurations CB-2C-6, CB-3C-1, and CB-4C-4 also have the same number of internal blanket assemblies. These three configurations are, therefore, different rearrangements of the same number of fuel and internal blanket assemblies to form tightly coupled cores. The sodium void reactivity varies very little for these cores. It is  $0.58\% \Delta k$  for CB-2C-6,  $0.57\% \Delta k$  for CB-3C-1, and  $0.61\% \Delta k$  for CB-4C-4. Thus, for a given number of internal blanket assemblies, the sodium void reactivity is roughly independent of the number of core zones in a tightly coupled core. We further demonstrate this result by considering configuration CB-6C-5, where a row of fuel assemblies is alternated with a row of blanket assemblies. The sodium void reactivity is  $0.52\% \Delta k$ , which is a very small decrease from the values of the previous cores in view of the fact that the total number of internal blanket assemblies has been increased from 169 to 234.

Configuration CB-3C-3 has been constructed from configuration CB-3C-1 by adding 18 internal blanket assemblies to internal blanket two and 30 internal blanket assemblies to internal blanket three. Thus, the neutronic coupling between the core zones has been decreased. As we have seen in the case of the loosely coupled cores this leads to a decrease in the sodium void reactivity. In this case the sodium void reactivity is  $0.37\% \Delta k$  which is significantly lower than all the other tightly coupled center blanket configurations. The degree of neutronic coupling is, therefore, far more important than the number of core zones into which the fuel assemblies are arranged.

Configuration CB-3C-2 is a variation of configuration CB-3C-1, in that the number of fuel and internal blanket assemblies per region are different. However, the total number of fuel assemblies and the total number of blanket assemblies are equal. The sodium void reactivity for this particular configuration was calculated by the direct eigenvalue method, and therefore

cannot be compared exactly with those of the other configurations which are results of perturbation theory calculations. We have seen that in general for heterogeneous cores perturbation theory underpredicts the sodium void reactivity with respect to a direct eigenvalue calculation by about 0.03 to 0.04%  $\Delta k$  for sodium void reactivities in the neighborhood of 0.6%  $\Delta k$ . If we apply this estimate to the result for configuration CB-3C-2, we see that the sodium void reactivities do not differ greatly. The slightly higher value can be attributed to the greater neutronic decoupling in configuration CB-3C-2 due to the removal of 6 internal blanket assemblies from internal blanket 2 and 6 internal blanket assemblies from internal blanket 3.

#### 4.2.2 Center Core Configurations

The core layouts for the tightly coupled center core configurations are shown in Fig. 17. There are three layouts with three core zones, CC-3C-1, CC-3C-2, and CC-3C-3, two with four core zones CC-4C-4, and CC-4C-6, and one with six core zones CC-6C-5. All the cores have a total of 360 fuel assemblies, with the exception of CC-3C-3 which has 366 fuel assemblies, and CC-4C-6 which has 468. The total number of blanket assemblies varies.

For the configurations with a 41 in. core height, the sodium void reactivities are given in Table X. The sodium void reactivities vary from 0.87%  $\Delta k$  for the three core zone configuration with 96 internal blanket assemblies to 0.58%  $\Delta k$  for the six core zone configuration with 210 internal blanket assemblies. This spread in the sodium void reactivities is somewhat larger than that for the configuration with a center blanket. This can be ascribed to some extent to the center core, whose sodium void reactivity is very sensitive to its size. However, as in the case of the loosely coupled cores, the overriding effect in the reduction of the sodium void reactivity comes from the decoupling of the core zones, as evident in configuration CC-3C-3, which has thicker internal blankets and therefore a lower sodium void reactivity than in configuration CC-3C-1.

#### 4.2.3 Core Height Variation

The approach used in determining the effect of core height reduction on the reduction of the sodium void reactivity is the same for the tightly coupled cores as it was for the loosely coupled cores. Since no significant difference is expected between the results for the center core and center blanket configurations, it suffices to consider only one, the center core configuration CC-3C-3. The sodium void reactivities for this configuration at three

different core heights (34, 41, and 52 in.) for the case when the power is fixed by changing the number of pins per assembly are given in Table XI. The sodium void reactivity varies from 0.78%  $\Delta k$  to 0.41%  $\Delta k$  as the core height is reduced from 52 in. to 34 in. This result is exactly analogous as in the case of the loosely coupled cores. The reduction in the sodium void reactivity is due to the increase in the axial leakage because of the reduction of the core height, and the decoupling of the core zones due to the increase in the internal blanket assembly size.

One other approach to maintain reactor power while reducing core height is to create an additional core zone with fuel assemblies. Configurations CC-3C-3 and CC-4C-6 have been constructed in such a manner. The total number of fuel assemblies in configuration CC-3C-3 is 366 and in CC-4C-6 it is 468 assemblies. As shown in Table XII the first two core zones and the first two internal blanket zones contain the same number of assemblies. In constructing configuration CC-4C-6 the third core zone of CC-3C-3 was reduced to two rows, then one row of internal blanket assemblies and two rows of fuel assemblies were added. This results in a core with a height of 32 in. and a reduction in the sodium void reactivity by a factor of two. If we compare this to the results in Table XI we see that the same reduction was also achieved by decreasing the core height to 34 in. and increasing the number of fuel pins per assembly from 271 to 331.

#### 4.2.4 Depletion Analysis Results

The six tightly coupled configurations which were deemed most promising in regard to sodium void reactivity were then carried through a depletion analysis as shown in Fig. 18. There are four center blanket configurations and two center core configurations. The tightly coupled cores at the reference core height of 41 in. have all shown BOL sodium void reactivities above \$1.50. This will lead to EOEC sodium void reactivities in excess of \$3.00, and consequently far in excess of the \$2.50 design limit in this study. We are, therefore, lead to consider only the 34 in. cores with 331 pins per fuel assembly in these cases.

The results for the tightly coupled center blanket configurations are given in Table XIII. The EOEC sodium void reactivities for voiding the core and the upper axial blanket of flowing sodium range from 0.45%  $\Delta k$  to 0.68%  $\Delta k$ . That is, they are all below \$2.00. The reactor doubling times range from 15.4 to 17.1 years. The latter doubling time is for configuration CB-6C-5, with

six core zones. This doubling time exceeds the others by at least a year. The sodium void reactivity for this configuration is  $0.55\% \Delta k$ , which is not the lowest. Thus, a tightly coupled configuration with alternating single rows of fuel and internal blanket assemblies shows no advantage over the rest of the configurations, other than the lowest burnup swing. However, heterogeneous cores in general have low burnup swings in comparison to homogeneous cores. None of the rest of the tightly coupled center blanket cores in Table XIII exhibit a clear overall superiority.

The results for the two tightly coupled center core configurations are shown in Table XIV. Configuration CC-3C-3 was analyzed at two core heights 41 in. and 34 in. with respectively 271 and 331 fuel pins per assembly. Configuration CC-4C-6 was analyzed at a core height of 32 in. and with 271 fuel pins per assembly. The lowest reactor doubling time is attained by CC-3C-3 at a 41 in. core height. However, the EOC sodium void reactivity is  $2.82$  and in excess of the design limit. At a core height of 34 in., this configuration has a reactor doubling time of 15.0 years and a sodium void reactivity of  $2.26$ . Both values lie within the design limits of this study. Configuration CC-4C-6, although it has the lowest sodium void reactivity of  $1.91$ , its reactor doubling time is 16.3 years.

#### 4.2.5 Intercomparison

In general, for both the tightly coupled center blanket and center core configurations, changing the number of core regions while maintaining the same degree of neutronic coupling does not significantly affect the sodium void reactivity. This appears to be more true in the case of the center blanket configurations than for the center core configurations. However, for both types of configurations the addition of internal blankets in a manner which leads to a greater neutronic decoupling between core regions decreases the sodium void reactivity. In addition, for both types of configurations core height reduction can be an effective means for the reduction of the sodium void reactivity.

On the basis of breeding performance and lower burnup swing no clear superiority is exhibited by either the tightly coupled center blanket or center core configurations.

#### 4.2.6 Sensitivity Analysis

##### 4.2.6.1 Enrichment Split

The above intercomparison showed that no clear superiority is exhibited by tightly coupled center blanket and center core configurations with respect to the design limits of sodium void reactivity and doubling time. However, it is well known that heterogeneous core configurations can exhibit extreme power peaking sensitivity to enrichment changes. In Table XV we compare the sensitivity of the peak power density change in the inner-most core zone to a 0.5% change in the enrichment of the inner-most and the outermost core zone, for configurations CC-3C-3, CB-3C-1, and CB-4C-4. It is clear from the table that the center core configuration exhibits a far greater sensitivity to changes in enrichment than the center blanket configurations. Although we have shown the results for only three configurations, from our studies of all the other configurations it is clear that for reasonable heterogeneous configurations this result is general.



## 5.0 CONCLUSIONS

This appendix has dealt with a comparative study of tightly and loosely coupled heterogeneous center core and center blanket configurations. Throughout this study we have kept these two types of configurations separate as much as possible in order to identify more clearly the generic issues which must be taken into account when constructing a radially heterogeneous core. Although, as the final configurations of this study show, the optimum cores with respect to the design constraints are a hybrid of tightly and loosely coupled, the following conclusions were instrumental in arriving at these configurations.

1. With respect to achieving a low sodium void reactivity and a low doubling time neither center core nor center blanket configurations show a clear advantage.
2. It is very difficult to construct a "reasonable" tightly or loosely coupled, center blanket or center core configuration with a \$2.00 sodium void reactivity at the EOEC. On the other hand cores with a \$3.00 limit on the sodium void reactivity can be readily constructed.
3. Center blanket configurations are less sensitive with regard to power peaking than center core configurations. In addition, 2-core zone configurations show a better burnup vs. power peaking performance than 3-core zone configurations.
- When a single enrichment is desirable a center core configuration leads to excessively high power peaking.
4. The sodium void reactivity contribution from the internal blanket assemblies on an assembly basis is significantly higher for tightly coupled cores than for loosely coupled cores.
5. Height reduction can be an effective means for reducing the sodium void reactivity for both tightly coupled and loosely coupled cores.
6. In general, primarily the configuration and not the number of internal blanket assemblies determines the sodium void reactivity.

7. In tightly coupled cores rearranging internal blankets to change the number of core zones does not significantly affect the sodium void reactivity.

8. Ranking configurations according to achievable sodium void reactivity favors loosely-coupled cores.

9. Ranking configurations according to breeding performance and power peaking sensitivity favors tightly-coupled cores.

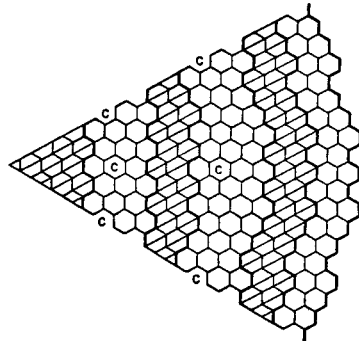
## 6.0 ACHIEVABLE SODIUM VOID REACTIVITIES

The tightly and loosely coupled cores, which can achieve sodium void reactivities of \$2.00, \$2.50, and \$3.00, for a two-year fuel residence time and multi-batch refueling, are shown in Table XVI. Forty inch loosely coupled cores with either a center blanket or a center core zone can be constructed with a lower limit on the sodium void reactivity of \$2.00. For tightly coupled cores this is true only for cores with a \$3.00 lower limit. If this limit is reduced to \$2.50, it becomes questionable whether this limit can be achieved at a core height of 40 in. For cores with a reduced core height this limit is attainable. For tightly coupled cores a \$2.00 sodium void reactivity is questionable even for cores shorter than 40 in.

This type of rough classification can also be made with respect to straight burn and multi-batch fuel management. Straight burn fuel management is more desirable from the standpoint of economics. However, an overview of Tables XVII and XVIII shows that with this type of fuel management, there are far fewer possible low sodium void cores than with multi-batch fuel management. Loosely coupled cores, with a core height less than 40 in. can achieve a \$2.00 sodium void reactivity, except for those with a three year or more straight burn cycle. At a core height of 40 in., this is only true up to a \$2.50 sodium void reactivity. With tightly coupled cores, as is shown in Table XVIII there are fewer options. For a 40 in. core height, only a \$3.00 limit can be achieved with some degree of certainty, and this only for a two year multi-batch fuel management. For cores which are shorter than 40 in. a \$2.50 sodium void reactivity is possible for a two year straight-burn and two and three year multi-batch fuel management.

# ASSEMBLIES

IC 114  
 OC 240  
 TOTAL CORE 354  
 CENTER BLANKET 55  
 INTERNAL BLANKET 114  
 TOTAL INTERNAL  
 BLANKET 169  
 S.V.C. 0.378%  $\Delta k$



IC 132  
 OC 222

TOTAL CORE 354  
 CENTER BLANKET 109  
 INTERNAL BLANKET 60  
 TOTAL INTERNAL BLANKET 169  
 S.V.C. 0.760%  $\Delta k$

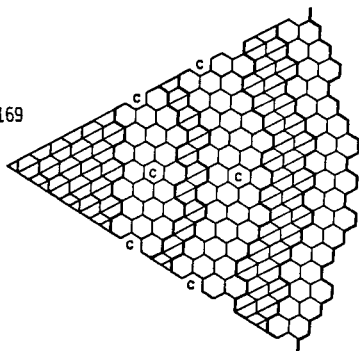


Fig. 1. Effect of Core Layout on Sodium Void Reactivity

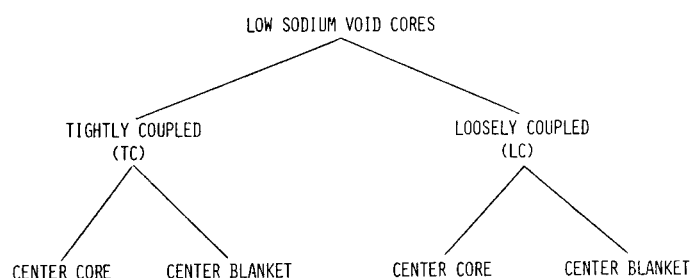


Fig. 2. Low Sodium Void Cores

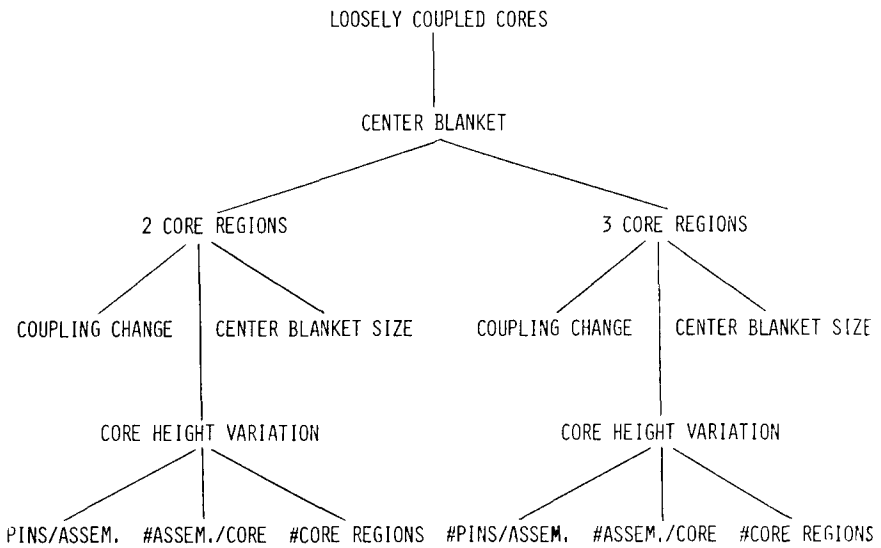


Fig. 3. Loosely Coupled Center Blanket Cores

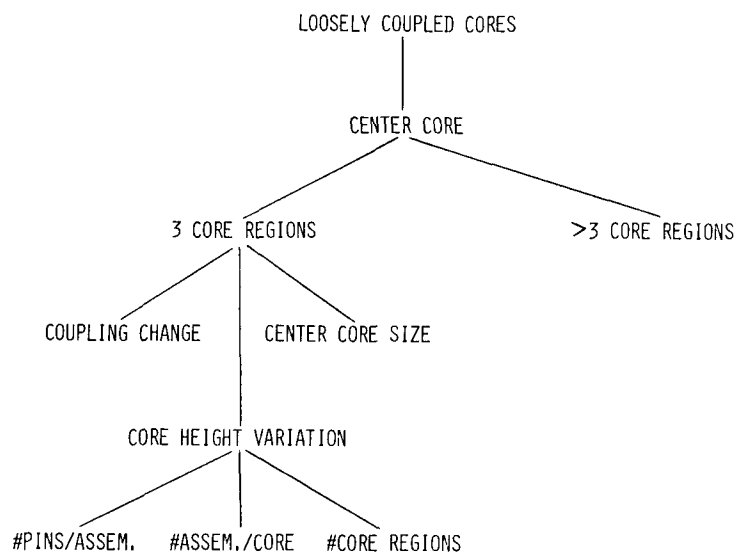


Fig. 4. Loosely Coupled Center-Core Cores

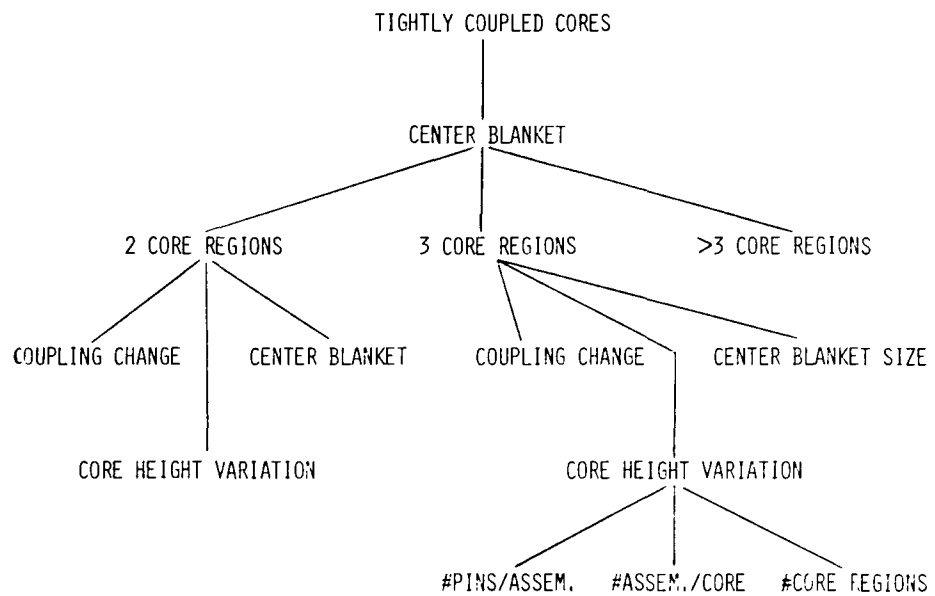


Fig. 5. Tightly Coupled Center-Blanket Cores

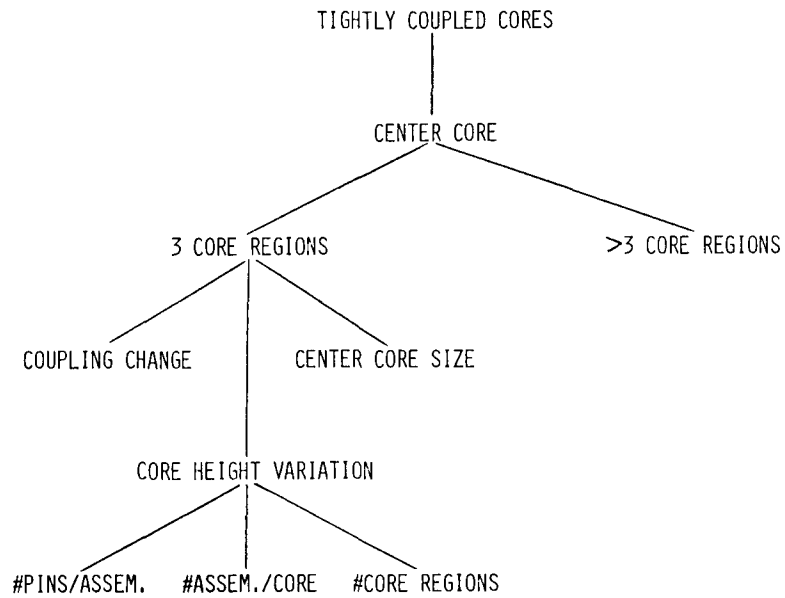


Fig. 6. Tightly Coupled Center-Core Cores

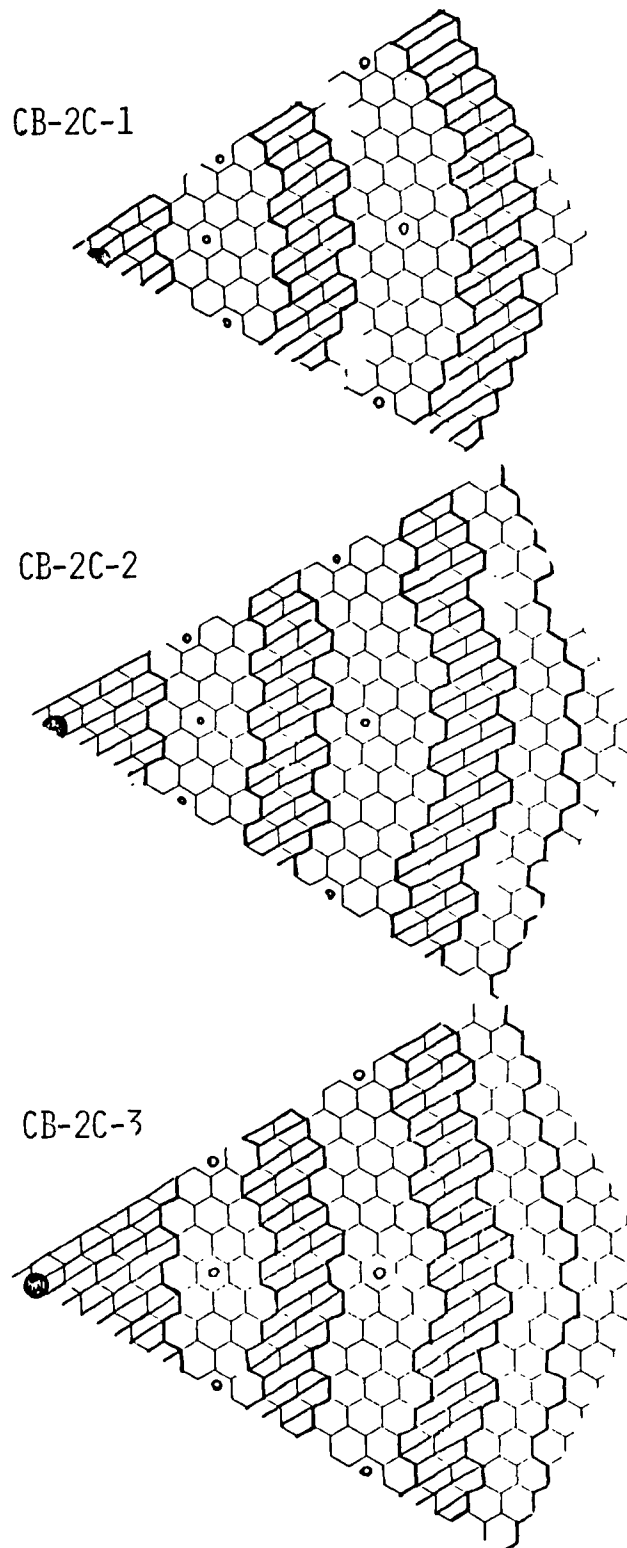


Fig. 7. Loosely-Coupled, Center-Blanket,  
Two Core Zones

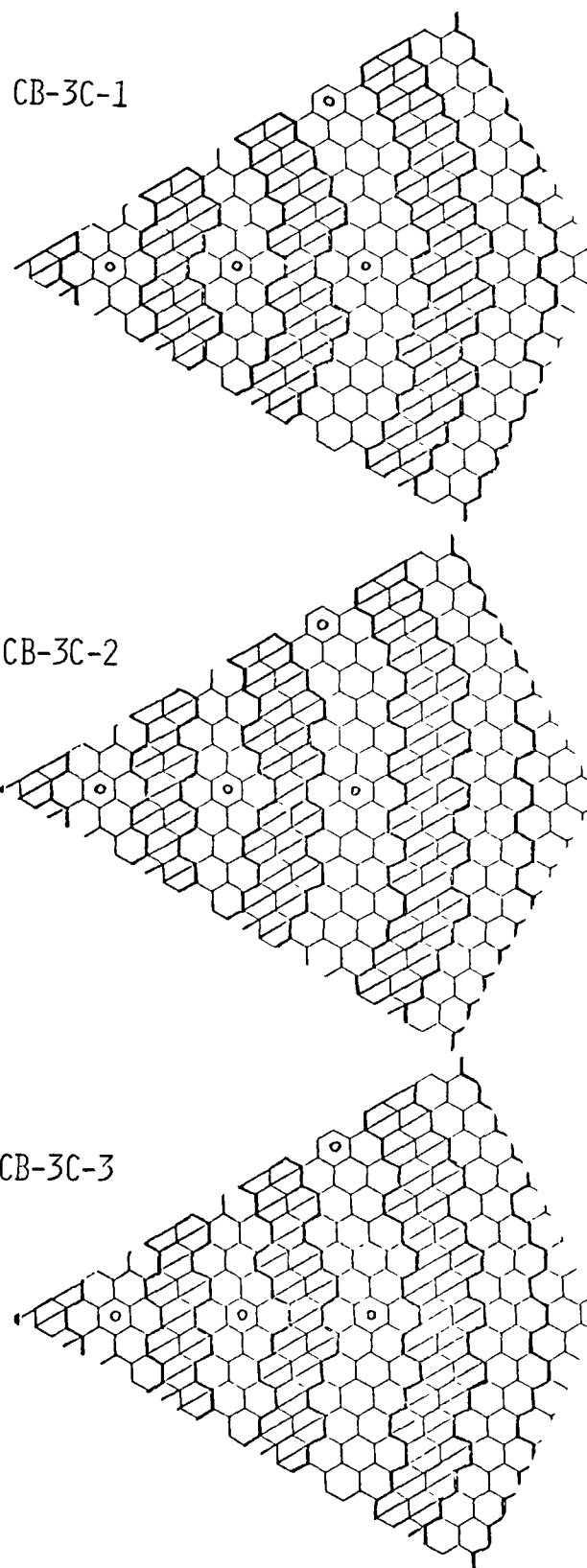


Fig. 8. Loosely-Coupled, Center-Blanket,  
Three Core Zones

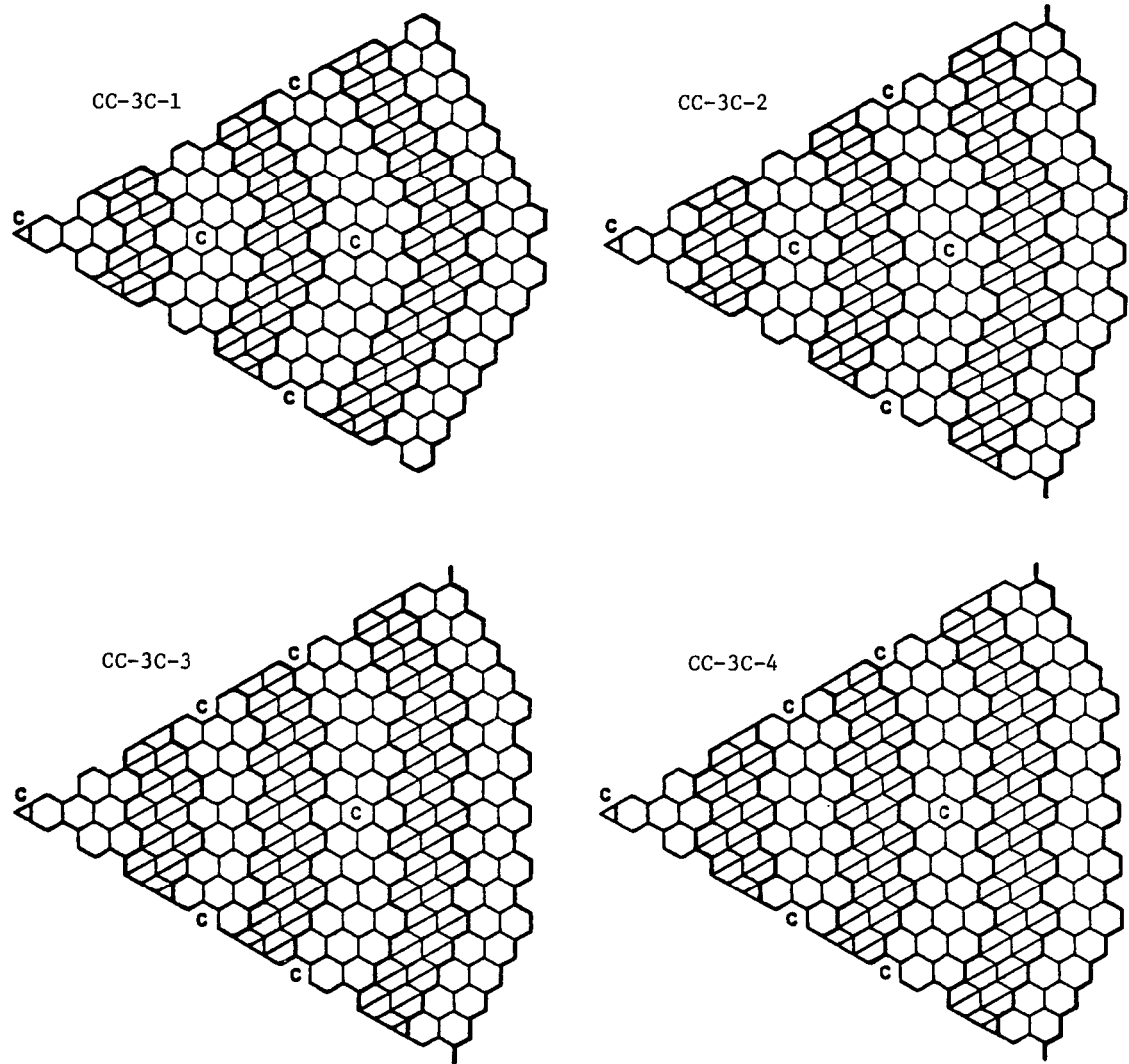


Fig. 9. Loosely-Coupled, Center-Core, Three Core Zones

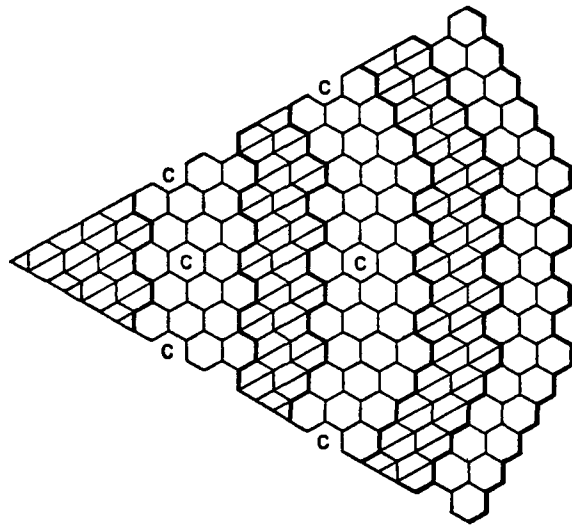


Fig. 10. Configuration for Core Height Reduction Evaluations

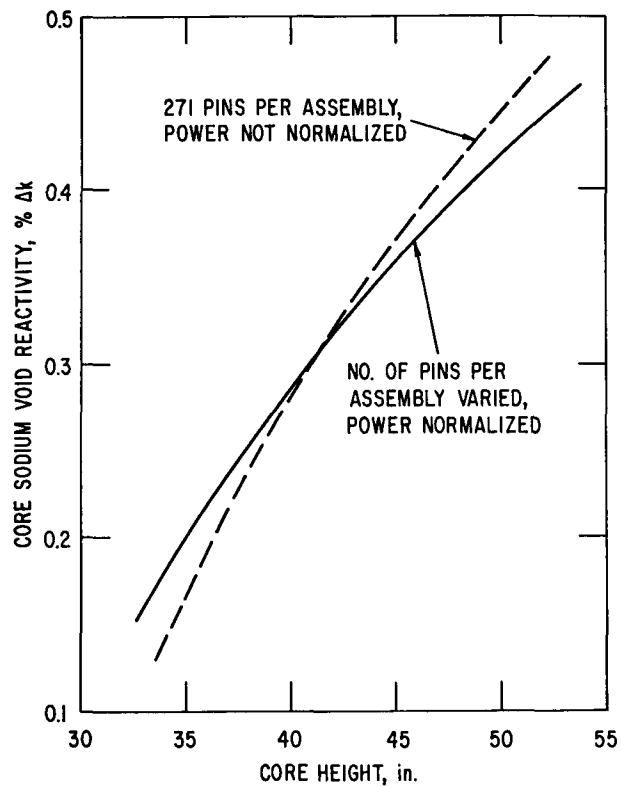
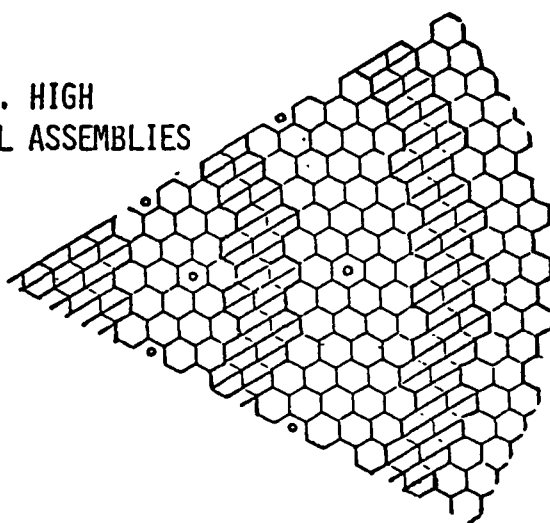
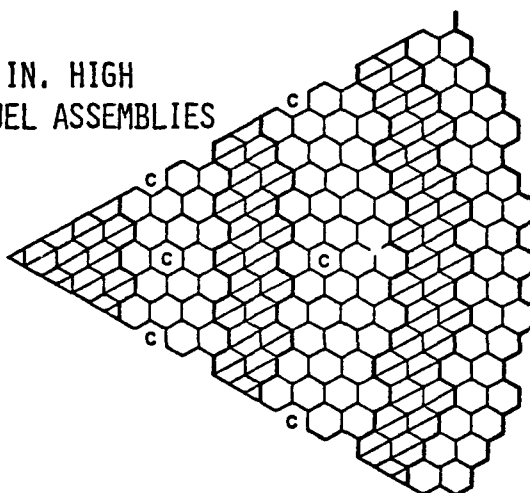


Fig. 11. Sodium Void Reactivity as a Function of Core Height

33.5 IN. HIGH  
456 FUEL ASSEMBLIES



41.73 IN. HIGH  
366 FUEL ASSEMBLIES



48 IN. HIGH  
318 FUEL ASSEMBLIES

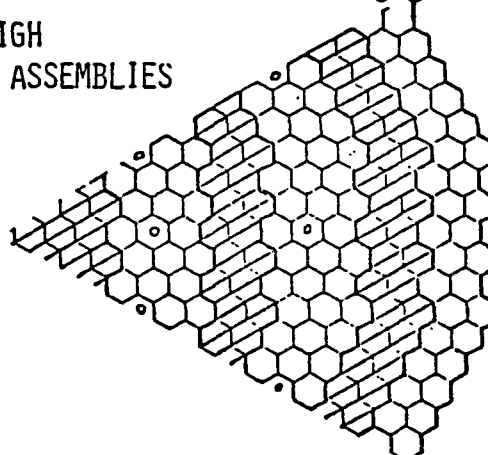


Fig. 12. Configurations for Three Different Core  
Heights (271 Pins per Assembly)

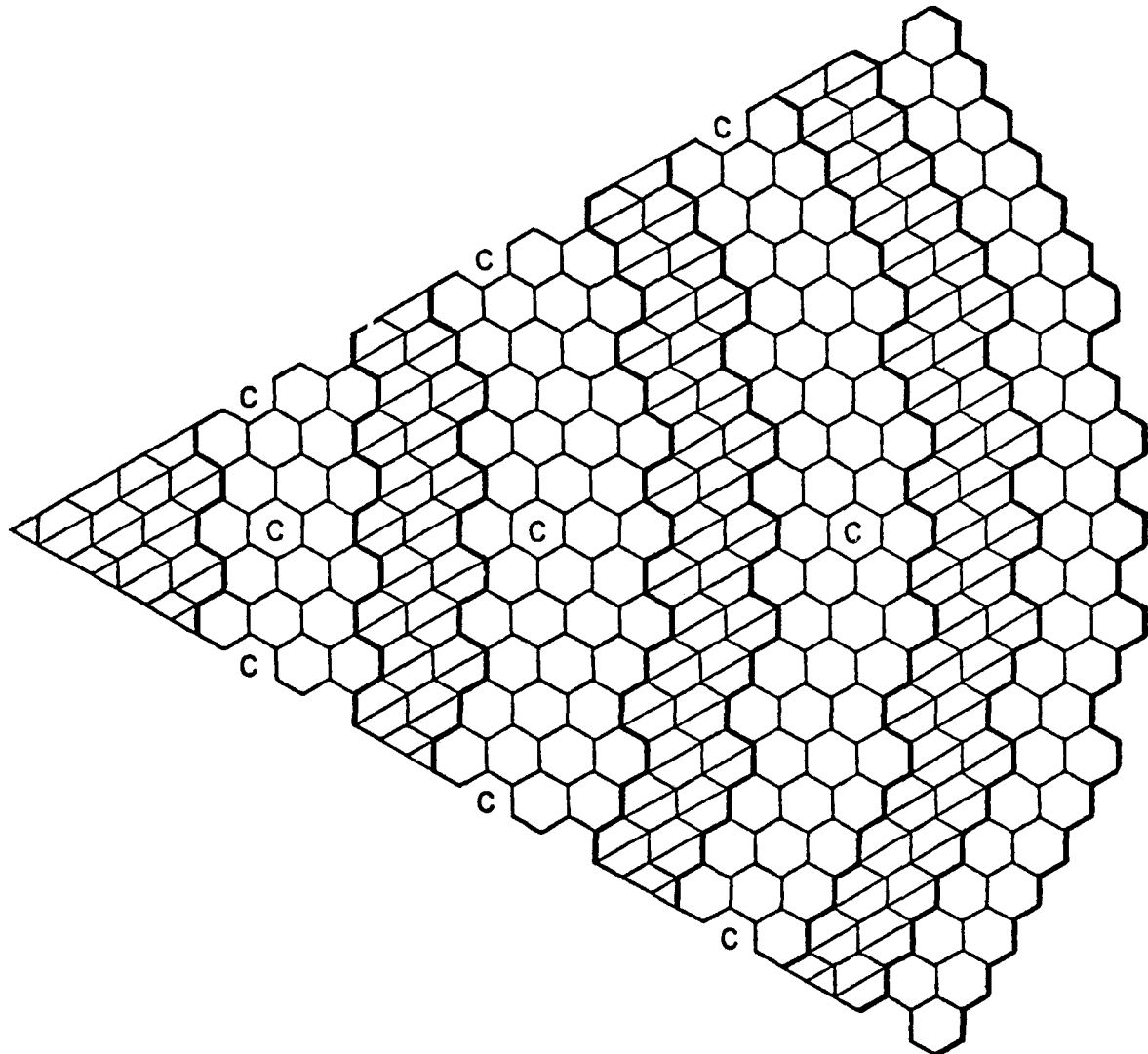


Fig. 13. Configuration for 22.53 in. High Core (271 Pins per Assembly)

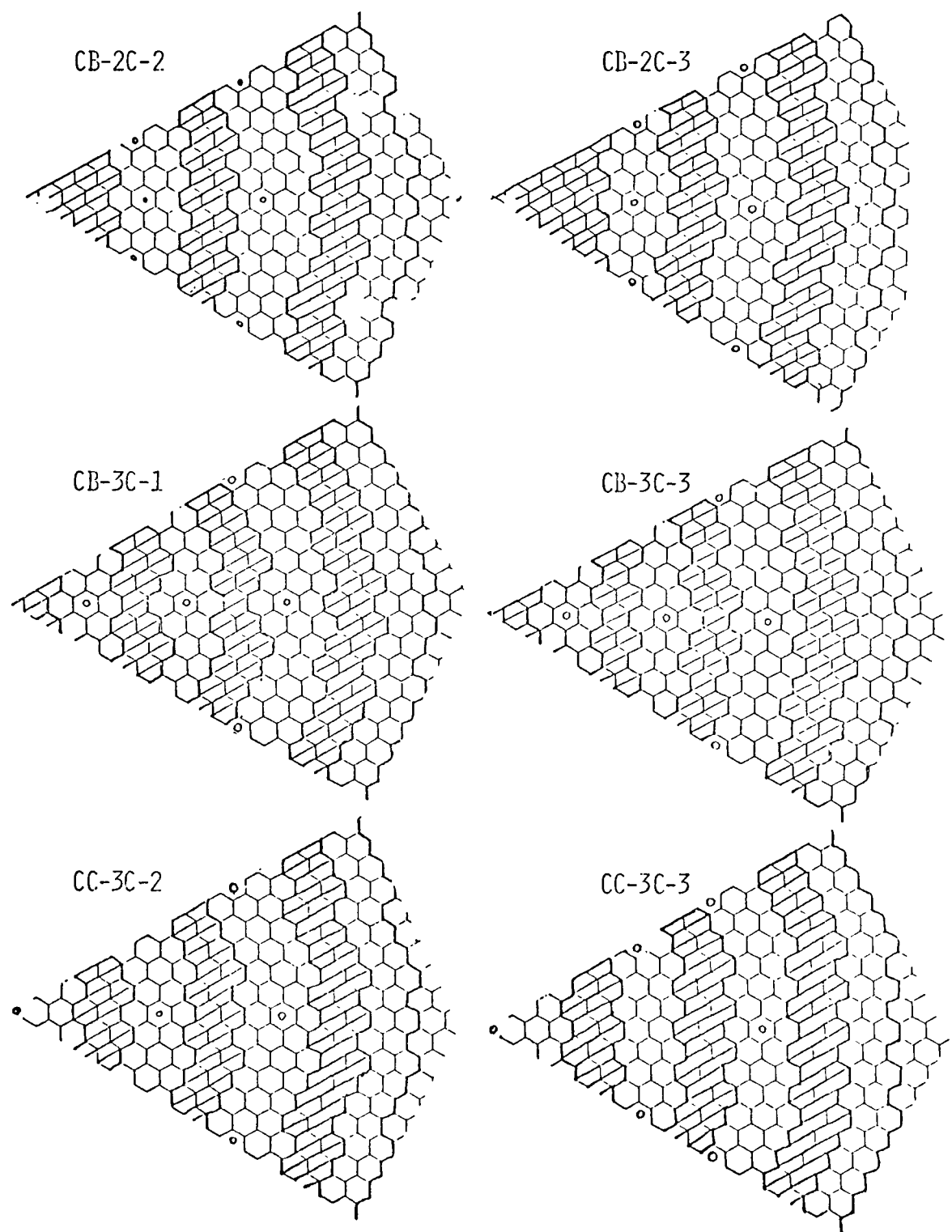


Fig. 14. Loosely-Coupled Configurations for Burnup Calculations

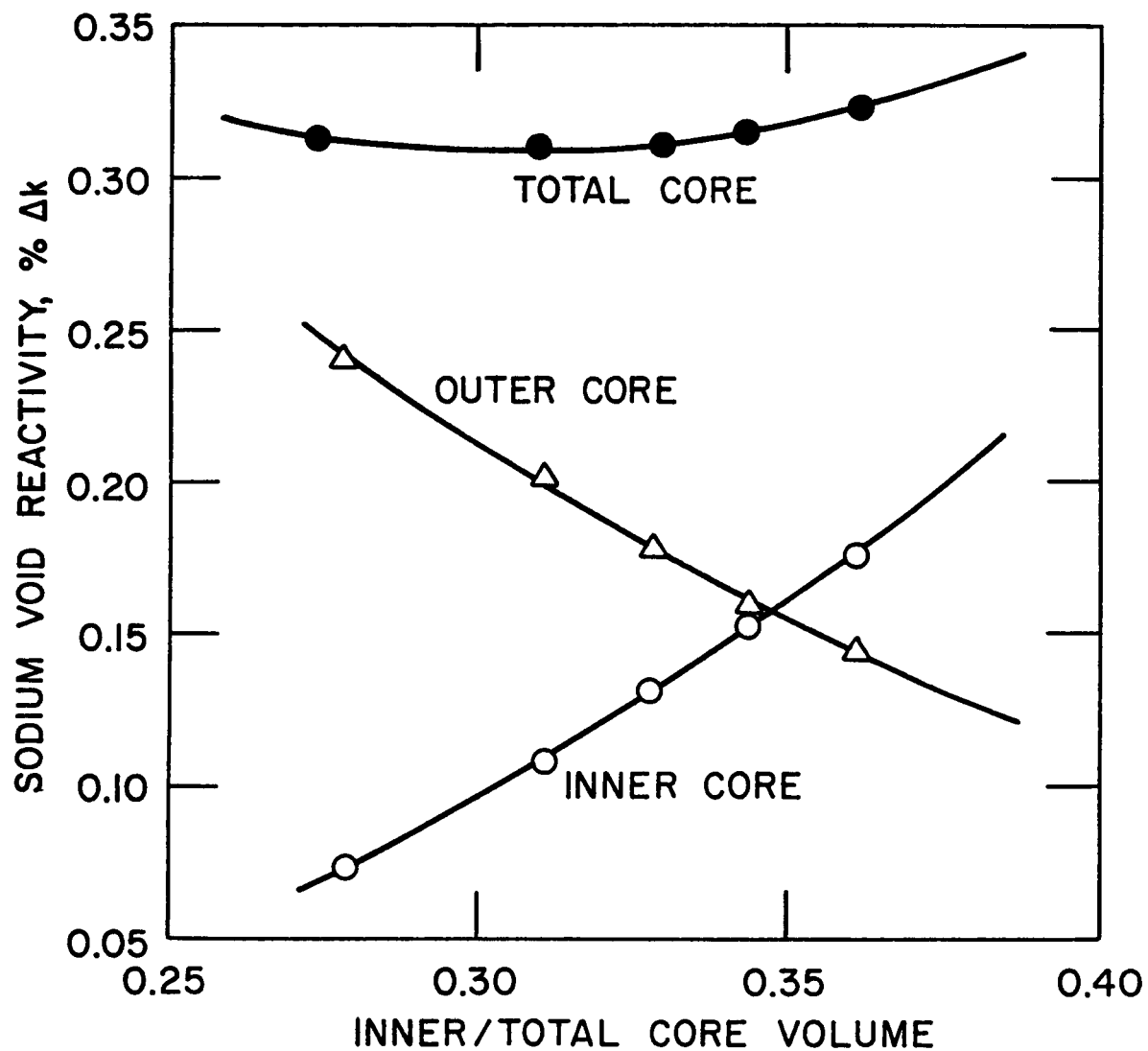


Fig. 15. Sodium Void Reactivity as a Function of Core Volume Split

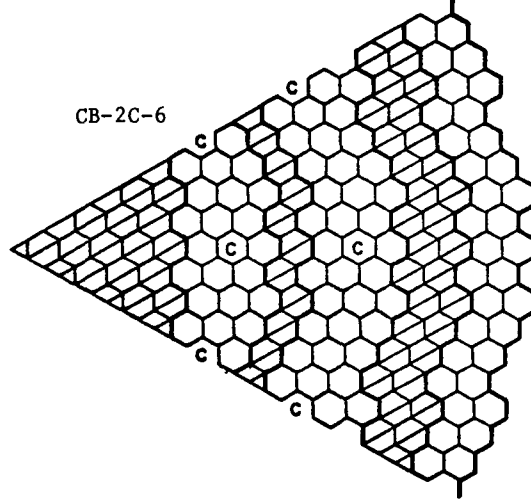
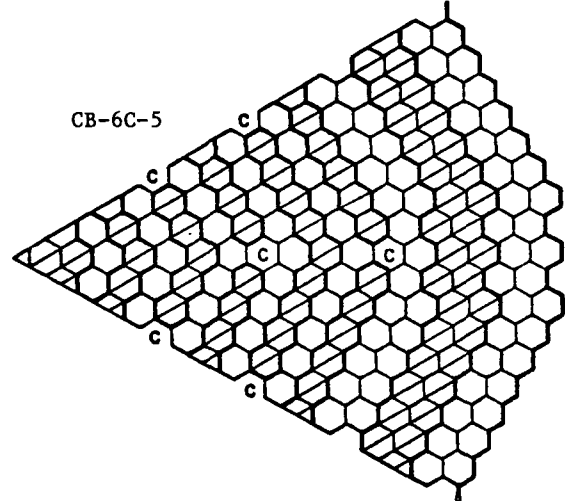
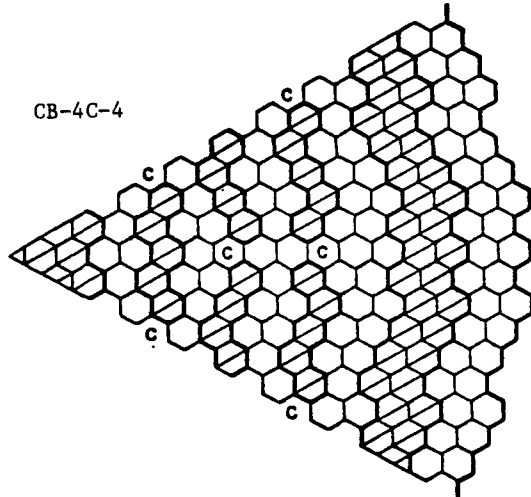
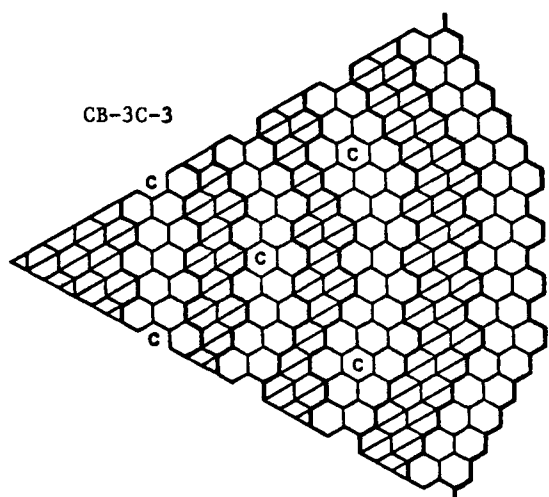
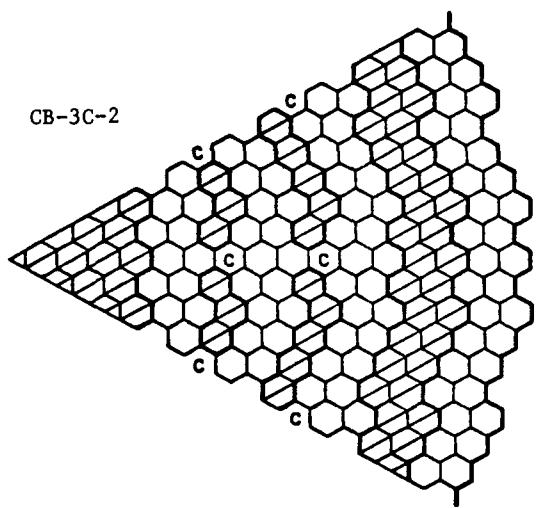
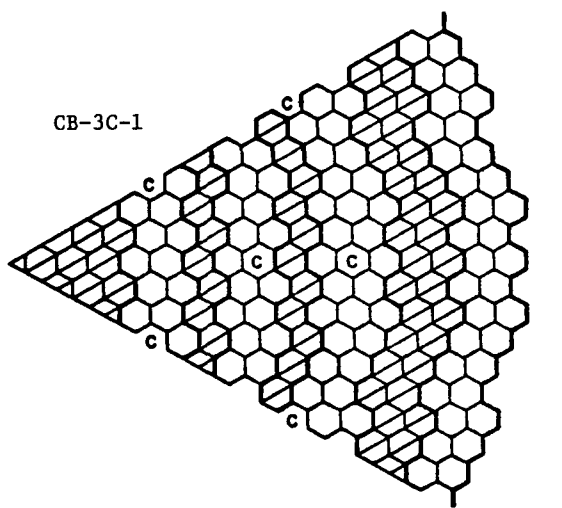


Fig. 16. Tightly Coupled Center Blanket Cores

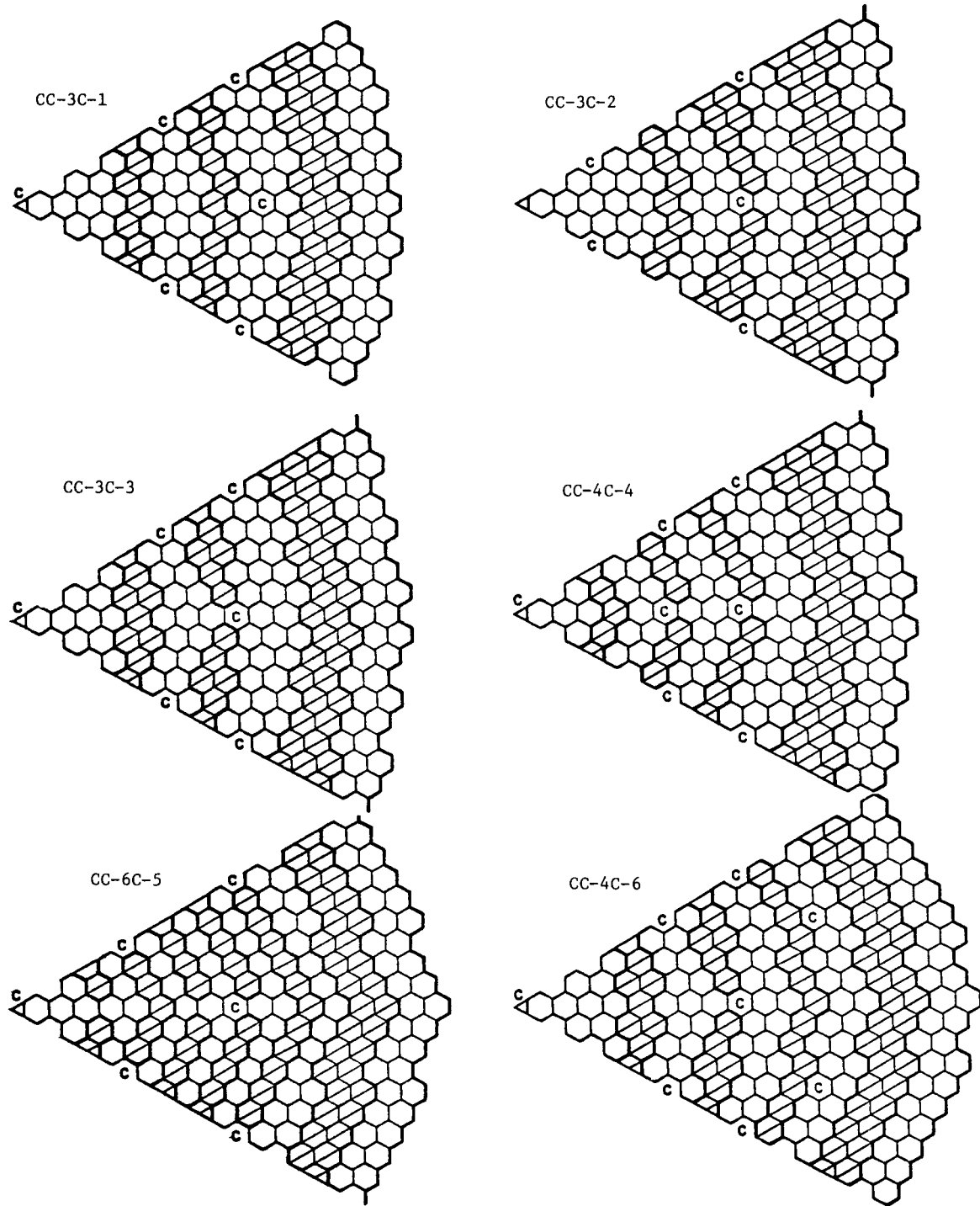


Fig. 17. Tightly Coupled Center-Core Cores

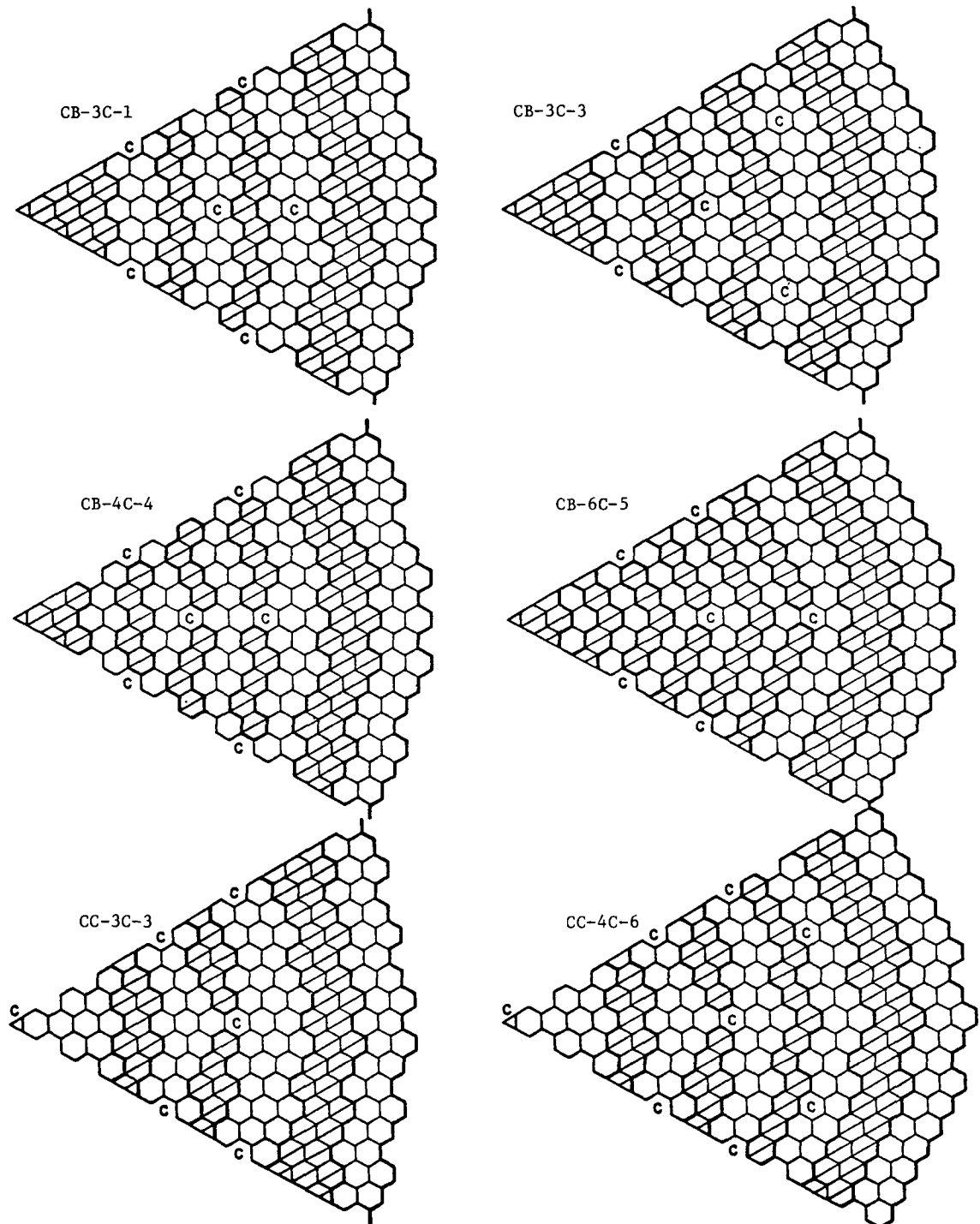


Fig. 18. Core Configurations for Depletion Analysis

TABLE I. Loosely-Coupled, Center-Blanket, Two Core Zones

Configuration	CB-2C-1	CB-2C-2	CB-2C-3
<b>Number of Assemblies</b>			
Inner Core	108	114	120
Outer Core	246	240	234
Total Core	354	354	354
Internal Blanket 1	31	55	91
Internal Blanket 2	102	114	126
Total Internal Blanket	133	169	217
<b>Effective Region Thickness, in.</b>			
Inner Core	21.33	19.16	17.12
Outer Core	21.26	19.72	18.13
Internal Blanket 1	17.67	23.54	30.28
Internal Blanket 2	11.48	11.81	11.90
Reactor Diameter, ft.	15.72	16.04	16.65
<b>BOL Sodium Void Reactivity, % <math>\Delta k</math></b>			
Inner Core	0.153	0.113	0.090
Outer Core	0.232	0.175	0.128
Total Core	0.385	0.288	0.218
Fissile Inventory, kg	4148	4328	4541

TABLE II. Loosely-Coupled, Center-Blanket, Three Core Zones

Configuration	CB-3C-1	CB-3C-2	CB-3C-3
<b>Number of Assemblies</b>			
Inner Core	54	54	54
Middle Core	102	102	102
Outer Core	198	198	198
Total Core	354	354	354
Internal Blanket 1	13	13	13
Internal Blanket 2	72	60	60
Internal Blanket 3	120	120	108
Total Internal Blanket	205	193	181
<b>Effective Region Thickness, in.</b>			
Inner Core	15.67	15.67	15.67
Middle Core	12.26	12.66	12.66
Outer Core	15.34	15.54	15.75
Internal Blanket 1	11.44	11.44	11.44
Internal Blanket 2	11.10	9.48	9.48
Internal Blanket 3	10.81	11.03	10.02
Reactor Diameter, ft.	16.55	16.44	16.35
<b>BOL Sodium Void Reactivity, % <math>\Delta k</math></b>			
Inner Core	0.060	0.083	0.081
Middle Core	0.096	0.115	0.135
Outer Core	0.064	0.062	0.087
Total Core	0.220	0.260	0.303
Fissile Inventory, kg	4978	4895	4826

TABLE III. Loosely-Coupled, Center-Core, Three Core Zones

Configuration	CC-3C-1	CC-3C-2	CC-3C-3	CC-3C-4
<b>Number of Assemblies</b>				
Inner Core	36	30	54	42
Middle Core	120	108	108	120
Outer Core	204	222	198	198
Total Core	360	360	360	360
Internal Blanket 1	48	54	66	66
Internal Blanket 2	114	114	126	126
Total Internal Blanket	162	168	192	192
<b>Effective Region Thickness, in.</b>				
Inner Core	16.13	14.50	20.36	17.64
Middle Core	16.84	15.51	13.74	15.52
Outer Core	16.61	18.08	15.54	15.54
Internal Blanket 1	9.96	11.59	11.37	12.32
Internal Blanket 2	11.11	11.38	11.65	11.65
Reactor Diameter, ft.	15.98	16.04	16.45	16.45
<b>BOL Sodium Void Reactivity, % <math>\Delta k</math></b>				
Inner Core	0.058	0.026	0.097	0.049
Middle Core	0.162	0.111	0.086	0.112
Outer Core	0.082	0.125	0.049	0.047
Total Core	0.302	0.262	0.232	0.208
Fissile Inventory, kg	4591	4628	4801	4770

TABLE IV. Effects of Core Height Reduction on Sodium Void Reactivity  
(Configuration Varied, Power Normalized)

Core Height, in.	No. of Fuel Assemblies	Pins/Assembly	Core Sodium Void Reactivity, % $\Delta k$
33.5	456	271	0.298
41.73	366	271	0.310
48	318	271	0.322

TABLE V. Loosely-Coupled, Center-Blanket, Two Core Zones

Configuration	CB-2C-2	CB-2C-2	CB-2C-3	CB-2C-3
Core Height, in.	41.73	34.16	41.73	34.16
No. of Pins per Fuel Assembly	271	331	271	331
No. of Assemblies				
Core Zone 1	114	114	120	120
Zone 2	240	240	234	234
Zone 3				
Total	354	354	354	354
Internal Blanket				
Zone 1	55	55	91	91
Zone 2	114	114	126	126
Zone 3				
Total	169	169	217	217
BOEC Fissile Inventory, kg	4995	5125	5235	5352
Burnup Swing, $\Delta k$	0.0210	0.0269	0.0214	0.0270
BOL Sodium Void Reactivities, <sup>a</sup> % $\Delta k$				
Core + Upper Axial Blanket	0.238		0.169	
Internal Blanket	0.058		0.057	
EOEC Sodium Void Reactivities, <sup>a</sup> % $\Delta k$				
Core + Upper Axial Blanket	0.672	0.497	0.579	0.409
Internal Blanket	0.105	0.057	0.106	0.055
Breeding Ratio (Equilibrium Cycle)	1.442	1.442	1.459	1.459
Reactor Doubling Time, years	15.4	15.9	15.6	16.1

<sup>a</sup>Flowing sodium only

TABLE VI. Loosely-Coupled, Center-Blanket, Three Core Zones

Configuration	CB-3C-1	CB-3C-1	CB-3C-3	CB-3C-3
Core Height, in.	41.73	34.16	41.73	34.16
No. of Pins per Fuel Assembly	271	331	271	331
No. of Assemblies				
Core Zone 1	54	54	54	54
Zone 2	102	102	102	102
Zone 3	198	198	198	198
Total	354	354	354	354
Internal Blanket				
Zone 1	13	13	13	13
Zone 2	72	72	60	60
Zone 3	120	120	108	108
Total	205	205	181	181
BOEC Fissile Inventory, kg	5541	5706	5352	5529
Burnup Swing, $\Delta k$	0.0105	0.0181	0.0083	0.0158
BOL Sodium Void Reactivities, <sup>a</sup> % $\Delta k$				
Core + Upper Axial Blanket	0.174		0.258	
Internal Blanket	0.171		0.194	
EOEC Sodium Void Reactivities, <sup>a</sup> % $\Delta k$				
Core + Upper Axial Blanket	0.576	0.381	0.671	0.475
Internal Blanket	0.233	0.157	0.252	0.183
Breeding Ratio (Equilibrium Cycle)	1.482	1.483	1.476	1.478
Reactor Doubling Time, years	15.8	16.3	15.4	15.9

<sup>a</sup>Flowing sodium only

TABLE VII. Loosely-Coupled, Center-Core, Three Core Zones

Configuration	CC-3C-2	CC-3C-2	CC-3C-3	CC-3C-3
Core Height, in.	41.73	34.16	41.73	34.16
No. of Pins per Fuel Assembly	271	331	271	331
No. of Assemblies				
Core Zone 1	30	30	42	42
Zone 2	108	108	120	120
Zone 3	222	222	198	198
Total	360	360	360	360
Internal Blanket				
Zone 1	54	54	66	66
Zone 2	114	114	126	126
Zone 3				
Total	168	168	192	192
BOEC Fissile Inventory, kg	5171	5322	5389	5539
Burnup Swing, $\Delta k$	0.0147	0.0219	0.0150	0.0223
BOL Sodium Void Reactivities, <sup>a</sup> % $\Delta k$				
Core + Upper Axial Blanket	0.213		0.160	
Internal Blanket	0.113		0.112	
EOEC Sodium Void Reactivities, <sup>a</sup> % $\Delta k$				
Core + Upper Axial Blanket	0.661	0.465	0.596	0.401
Internal Blanket	0.174	0.107	0.169	0.102
Breeding Ratio (Equilibrium Cycle)	1.466	1.466	1.474	1.473
Reactor Doubling Time, years	15.1	15.7	15.6	16.1

<sup>a</sup>Flowing sodium only

TABLE VIII. Loosely Coupled Cores  
 Power Peaking Sensitivity on Enrichment Changes  
 (BOL Conditions)

Configuration	Peak Power Density Change in Inner-Most Core Zone, %		
	CB-2C-2	CB-3C-3	CC-3C-2
0.5% Change in Enrichment of Inner- Most Core Zones	5.6	5.3	7.0
0.5% Change in Enrichment of Outer- Most Core Zone	5.4	5.4	8.2

TABLE IX. Center Blanket Tightly Coupled Cores

Configuration	CB-2C-6	CB-3C-1	CB-3C-2	CB-3C-3	CB-4C-4	CB-6C-5
Core Height, in.	41	41	41	41	41	41
Number of Assemblies						
Core 1	132	72	78	72	42	--
Core 2	222	108	114	108	60	--
Core 3	--	174	162	174	102	--
Core 4	--	--	--	--	150	--
Total Core	354	354	354	354	354	354
Internal Blanket 1	109	55	73	55	31	--
Internal Blanket 2	60	48	36	66	30	--
Internal Blanket 3	--	66	60	96	48	--
Internal Blanket 4	--	--	--	--	60	--
Total Internal Blanket	169	169	169	217	169	234
BOL Sodium Void Reactivity <sup>a</sup> , % Δk						
Core 1	0.28	0.12	--	0.08	0.06	--
Core 2	0.30	0.31	--	0.21	0.16	--
Core 3	--	0.14	--	0.08	0.30	--
Core 4	--	--	--	--	0.09	--
Total Core	0.58	0.57	0.67 <sup>b</sup>	0.37	0.61	0.52
Fissile Inventory, kg	4009.0	4480.1	4363.7	4866.7	4675.2	5417.9

<sup>a</sup>Flowing sodium only<sup>b</sup>Direct eigenvalue calculation

TABLE X. Tightly Coupled Center Core Configurations

Configuration	CC-3C-1	CC-3C-2	CC-3C-3	CC-4C-4	CC-6C-5
Core Height, in.	41	41	41	41	41
Number of Assemblies					
Core 1	72	114	72	36	--
Core 2	108	102	102	60	--
Core 3	180	144	192	96	--
Core 4	--	--	--	168	--
Total Core	360	360	366	360	360
Internal Blanket 1	36	42	48	24	--
Internal Blanket 2	60	78	66	36	--
Internal Blanket 3	--	--	--	--	--
Total Internal Blanket	96	120	114	114	210
BOL Sodium Void Reactivity <sup>a</sup> , % Δk					
Core 1	0.52	0.49	0.23	0.13	--
Core 2	0.27	0.21	0.22	0.17	--
Core 3	0.08	0.05	0.17	0.29	--
Core 4	--	--	--	0.14	--
Total Core	0.87	0.76	0.62	0.74	0.58
Fissile Inventory, kg	4,194.3	4,469.3	4,347.5	4,443.4	5,405.4

<sup>a</sup>Flowing sodium only

TABLE XI. Core Height Variation of a Tightly Coupled Center Core Configuration

Configuration	CC-3C-3		
Core Height, in.	34	41	52
Number of Pins per Core Assembly	331	271	217
Number of Assemblies			
Core 1	72	72	72
Core 2	102	102	102
Core 3	192	192	192
Core 4	--	--	--
Total Core	366	366	366
Internal Blanket 1	48	48	48
Internal Blanket 2	66	66	66
Internal Blanket 3	--	--	--
Total Internal Blanket	114	114	114
BOL Sodium Void Reactivity <sup>a</sup> , % Δk			
Core 1	0.16	0.23	0.27
Core 2	0.14	0.22	0.29
Core 3	0.11	0.17	0.22
Total Core	0.41	0.62	0.78
Fissile Inventory, kg	4,457.3	4,347.5	4,284.8

<sup>a</sup>Flowing sodium only

TABLE XII. Core Height Variation with a Change  
in the Number of Core Zones

Configuration	CC-3C-3	CC-4C-6
Core Height, in.	41	32
Number of Assemblies		
Core 1	72	72
Core 2	102	102
Core 3	192	132
Core 4	--	162
Total Core	366	468
Internal Blanket 1	48	48
Internal Blanket 2	66	66
Internal Blanket 3	--	66
Total Internal Blanket	114	192
BOL Sodium Void Reactivity <sup>a</sup> , % $\Delta k$		
Core 1	0.23	0.14
Core 2	0.22	0.11
Core 3	0.17	0.16
Core 4	--	0.00
Total Core	0.62	0.40
Fissile Inventory, kg	4,347.5	5,038.3

<sup>a</sup>Flowing sodium only

TABLE XIII. Tightly Coupled Core Intercomparison

Configuration	CB-3C-1	CB-3C-3	CB-4C-4	CB-6C-5
Core Height, in.	34	34	34	34
No. of Pins per Fuel Assembly	331	331	331	331
No. of Assemblies				
Core Zone 1	72	72	42	--
Zone 2	108	108	60	--
Zone 3	174	174	102	--
Zone 4	--	--	150	--
Total	354	354	354	354
Internal Blanket				
Zone 1	55	55	31	--
Zone 2	48	66	30	--
Zone 3	66	96	48	--
Zone 4	--	--	60	--
Total	169	217	169	234
BOEC Fissile Inventory, kg	5283.8	5714.2	5470.3	6251.2
Burnup Swing, $\Delta k$	0.011	0.014	0.007	0.003
BOL Sodium Void Reactivities <sup>a</sup> , $\% \Delta k$				
Core				
EOEC Sodium Void Reactivities <sup>a</sup> , $\% \Delta k$				
Core + Upper Axial Blanket	0.66	0.45	0.65	0.55
Internal Blanket	0.22	0.20	0.25	0.35
Reactor Doubling Time, yrs.	15.4	16.1	15.5	17.1

<sup>a</sup>Flowing sodium only

TABLE XIV. Tightly Coupled Core Intercomparison

Configuration	CC-3C-3	CC-3C-3	CC-4C-6
Core Height, in.	41	34	32
No. of Pins per Fuel Assembly	271	331	271
No. of Assemblies			
Core Zone 1	72	72	72
Zone 2	102	102	102
Zone 3	192	192	132
Zone 4	--	--	162
Total	366	366	468
Internal Blanket			
Zone 1	48	48	48
Zone 2	66	66	66
Zone 3	--	--	78
Total	114	114	192
BOEC Fissile Inventory, kg	4,838.0	5026.9	5528.4
Burnup Swing, $\Delta k$	0.0064	0.0136	0.0079
BOL Sodium Void Reactivities <sup>a</sup> , % $\Delta k$			
Core	0.62	0.44	0.41
EOEC Sodium Void Reactivities <sup>a</sup> , % $\Delta k$			
Core + Upper Axial	0.99	0.79	0.67
Internal Blanket	0.21	0.16	0.28
Reactor Doubling Time, yrs.	14.4	15.0	16.3

<sup>a</sup>Flowing sodium only

TABLE XV. Tightly Coupled Cores Power  
Peaking Sensitivity to Enrichment Changes  
(BOL Conditions)

Configuration	Peak Power Density Change in Inner-most Core Zone, %		
	CC-3C-3	CB-3C-1	CB-4C-4
0.5% Change in Enrichment of Inner-most Core Zone	5.6	2.6	2.1
0.5% Change in Enrichment of Outer-most Core Zone	5.2	4.7	2.1

TABLE XVI. Achievable Sodium Void Reactivities  
(Two-Year Residence Time, Multi-Batch Refueling)

	Tightly Coupled				Loosely Coupled			
	Center Blanket		Center Core		Center Blanket		Center Core	
	40 in.	< 40 in.	40 in.	< 40 in.	40 in.	< 40 in.	40 in.	< 40 in.
≤ \$2.00	-	+(?)	-	+(?)	+	+	+	+
≤ \$2.50	-(?)	+	-(?)	+	+	+	+	+
≤ \$3.00	+	+	+	+	+	+	+	+

TABLE XVII. Loosely Coupled Cores

	40 in.				< 40 in.			
	Straight Burn		Multi-Batch		Straight Burn		Multi-Batch	
	3 Year	2 Year	3 Year	2 Year	3 Year	2 Year	3 Year	2 Year
≤ \$2.00	-	+ (?)	+ (?)	+	-	+	+	+
≤ \$2.50	-	+	+	+	+	+	+	+
≤ \$3.00	+	+	+	+	+	+	+	+

TABLE XVIII. Tightly Coupled Core

	40 in.				< 40 in.			
	Straight Burn		Multi-Batch		Straight Burn		Multi-Batch	
	3 Year	2 Year	3 Year	2 Year	3 Year	2 Year	3 Year	2 Year
≤ \$2.00	-	-	-	-	-	- (?)	- (?)	+ (?)
≤ \$2.50	-	-	-	- (?)	-	+	+	+
≤ \$3.00	-	+ (?)	+ (?)	+	+	+	+	+